6-2011

From Gene to Behavior: Investigation of Ppt1 and Ppt2 RNAi induced knock-down during Drosophila neurogenesis

Patrick J. O'Hern
Union College - Schenectady, NY

From Gene to Behavior: Investigation of Ppt1 and Ppt2 RNAi induced knock-down during *Drosophila* neurogenesis

By

Patrick O'Hern

****

Submitted in partial fulfillment
of the requirements for
Honors in the Department of Biology

UNION COLLEGE
June, 2011

ABSTRACT

O'HERN, PATRICK From Gene to Behavior: Investigation of Ppt1 and Ppt2 RNAi induced knock-down during *Drosophila* Neurogenesis, June 2011.

ADVISOR: Quynh Chu-LaGraff

Infantile Neuronal Ceroid Lipofuscinosis (INCL) is caused by a mutation of the gene CLN1, which encodes palmitoyl protein thioesterase 1 (PPT1). PPT1 is a lysosomal enzyme that cleaves the thioester bond connecting long chain fatty acids of palmitoylated proteins. Without PPT1, palmitoylated proteins are not degraded properly and this causes unwanted build up in neurons leading to fatality. Recently, it has been thought that a mutation in a similar enzyme, palmitoyl-protein thioesterase 2 (PPT2), another lysosomal hydrolase, may also be responsible for INCL by causing a similar effect of Ppt1 deficiency. A bioinformatics analysis in this study showed similarities between human PPT1/PPT2 and Drosophila Ppt1/Ppt2. Therefore, using Drosophila melanogaster as a model, the role of Ppt1 and Ppt2 can be elucidated using the molecular genetic technique RNA interference (RNAi). RNAi targets the mRNA for destruction thus creating a mutant phenotype. In this study, knock-down of Ppt1 and Ppt2 mRNA expression was achieved using the Gal4-AUS system. Transgenic Ppt1-UAS and Ppt2-UAS fly lines were crossed into various Gal4 driver lines specific for different subsets of embryonic CNS neurons. Embryos from these crosses were immunohistochemically stained with FAS II antibody and stage 16 embryos were examined for neural defects. Preliminary results indicate that Ppt1 and Ppt2 RNAi knock-down disrupted nervous system development in Drosophila. Furthermore, mutant embryos were allowed to progress to a larval state where motor studies showed differences in locomotor ability. These results provide insights into the mechanism of Ppt1 and Ppt2 in causing INCL pathology.

ACKNOWLEDGEMENTS

I would first like to thank Professor Chu-LaGraff for affording me the opportunity to work on this project during two summer research fellowships, an independent study and throughout this academic year. She not only guided me through this research, but has also helped me navigate the graduate school application process. I would also like to thank the Union College Biology Department Faculty and Union College Internal Education Fund for supporting this project and the chance to present this research at the Experimental Biology Conference in Washington D.C.. Thank you to the Fly base and the Vienna *Drosophila* RNAi Stock Center for the fly lines necessary for this research project. Finally, thank you to my friends and family for their support and visits to the basement.

TABLE OF CONTENTS

TABLE OF FIGURES

Figure Page

INTRODUCTION

NEURONAL CEROID LIPOFUSCINOSiS

Neuronal Cerioid Lipofuscinosis includes a group of rare lysosomal storage disorders. It is very rare as it effects only 0.1 to 7 per 100,000 live births each year. NCLs are inherited in an autosomal recessive manner meaning that if Mendilian genetics is applied it can be assumed that if both parents are carriers one of four children will be normal, two of four children will be carriers and one of four children will manifest the disease (see Figure 1) (5).

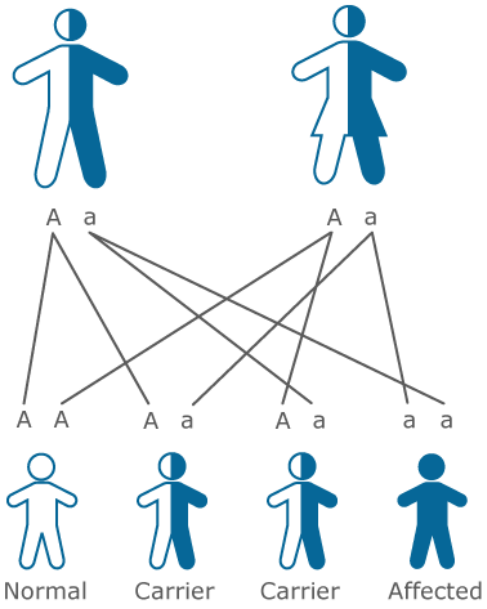

Figure 1: Genetics of autosomal recessive disorders and diseases (http://www.discern-genetics.org/images/6.1.gif)

NCLs are grouped into eight different categories: infantile classic NCL, late infantile classic NCL, juvenile classic NCL, adult NCL, Finish variant late infantile NCL, variant late infantile NCL, variant late infantile NCL, and Northern epilepsy/progressive epilepsy with mental retardation (EPMR). Each NCL case is grouped into one of these

categories based on the gene causing the disorder; so far six genes have been discovered that cause human NCL: CLN1, CLN2, CLN3, CLN5, CLN6, CLN8 (17). Table 1 outlines the known disorders and their corresponding genetic location and products.

Clinical types	Genetic types	Chromosomal loci	Gene product
EO-NCL	CLN10/ CTSD	not known	Not known
I-NCL	CLN1	Ip32	Lysosomal palmitoy1 Protein thioesterase
LI-NCL	CLN2	11p15	Lysosomal pepstatin Insensitive peptidase
LI-NCL	CLN5	13q31-32	Not known
J-NCL	CLN3	16p12	Transmembranous (?)
A-NCL	CLN4	not known	Not known
EJ-NCL	CLN6	15q21-23	Not known
tLI-NCL	CLN7	not known	Not known
vLI-NCL	CLN8	not known	Not known

I-NCL - Infantile NCL; LI-NCL - Late infantile NCL; J-NCL - Juvenile NCL; A-NCL - Adult NCL; EJ-NCL = Early juvenile NCL; EO-NCL: Early onset NCL

Table 1: A summary of the different genes involved in NCL along with the clinical disorders, chromosomal loci and gene products (19).

Currently, diagnosing these disorders is difficult given their overlapping pathology. The first sign of any NCL is generally retinal degeneration and ophthalmologists are generally the first to notice the loss of cells in the retina. From here, patients with a suspected NCL disorder undergo blood tests, skin sampling, brain scans, and electroencephalograms to confirm (16). Furthermore, genetic screening has recently become available for those NCLs that have been cloned (13). The present study shows, however, that it is possible other genes than those identified by the current literature may

be involved in NCLs. Presently, there is no treatment for any of the disorders other than symptomatic treatment (9).

INFANTILE NEURONAL CEROID LIPOFUSCINOSIS (INCL)

INCL is responsible for 20% to 25% of all NCL cases. The symptoms generally become apparent around six months of age and include retarded head growth, low muscle tone, and hyperexcitability. This condition is progressive and as age increases, patients typically experience cognitive dysfunction, blindness, loss of motor skills, and seizures. The average lifespan of an INCL patient is between 6 and 13 years (9).

INCL is caused by a mutation of the CLN1 gene, which encodes palmitoyl protein thioesterase 1 (PPT1). PPT1 is a lysosomal enzyme responsible for cleaving the thioester bond that connects long chain fatty acids of palmitoylated proteins (15). The most common fatty acid cleaved by the actions of PPT1 is palmitate. The active site of PPT1 includes a catalytic triad made up of: aspartate (Asp233), histidine (His289) and serine (Ser115) (1).

The CLN1 gene has a chromosomal location of 1p32 and 9 exons. In INCL cases, there have been 40 different mutation locations within CLN1 that have been identified in INCL patients. The various mutations are as follows: 19 missence mutations that alter amino acid residues, 9 nonsense mutations that delete HIS289 (the histidine of the active site) and cause a loss of enzymatic activity, 9 small deletions or insertions, and 3 mutations in splice sites which decrease enzymatic activity due to resulting geometric changes in the PPT1 active site (13).

Without PPT1, the palmitoylated proteins are never degraded and build up in the cell. This build up is thought to be the cause for the neurodegeneration seen in INCL

patients (5). Interestingly, while the build up of storage material occurs in cells ubiquitously, the only detrimental effects occur in neural cells (1). Therefore, there must be a process or component specific to neural cells that is disrupted by the accumulation of storage material. Unfortunately, current research has not shown exactly what this necessary factor is and it remains one of the large mysteries of this disorder (11).

CLN1 also encodes Ppt2, another gene responsible for catalyzing the hydrolysis of long chain fatty acyl CoAs and preventing unwanted build up of storage materials within the cell. Despite their similarities in function, Ppt2 only shares an 18% identity to Ppt1 and they are thought to perform non-redundant roles (see Figure 2) (21). Furthermore, in an experiment with Ppt1 and Ppt2 knock-out mice, the Ppt1 mice experienced more severe NCL-like symptoms than the Ppt2 mice. This suggests that Ppt2 serves a separate role than Ppt1, but nevertheless causes the same kind of autofluorescent storage material buildup characteristic of INCL (10).

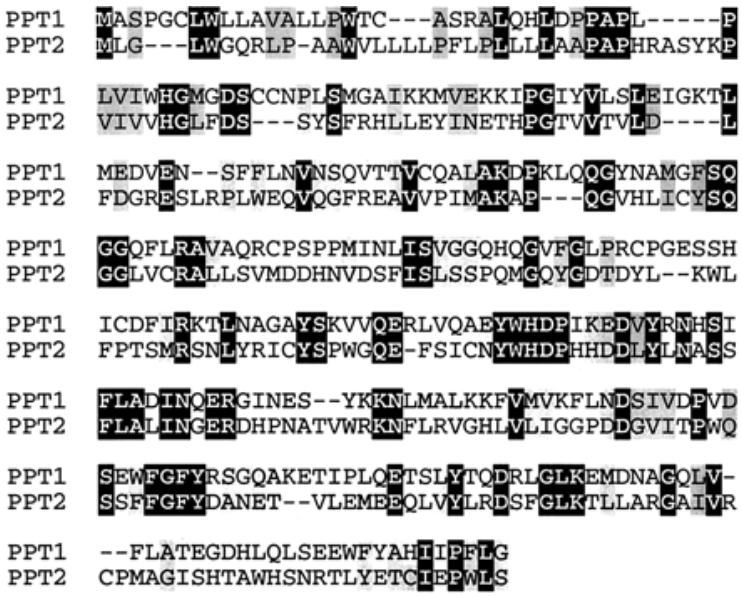

Figure 2: A PPT1 and PPT sequence comparison. Black sections represent identical residues and gray represents conserved substitutions (2).

The undegraded proteins that result from Ppt1 mutation and Ppt2 mutation may are better known as granular osmiophillic deposits (GRODs). Despite the fact that these GRODs are expressed ubiquitously throughout the human body, it is only the nervous system that appears to be affected. The build up of GRODs in neural cells can trigger the apoptosis of the central nervous system, which is responsible for the symptoms and prognosis of INCL (16).

Recent findings have shed some light on how GRODs cause apoptosis of neural cells. GRODs are made up of saposins A and D and build up in the endoplasmic reticulum. The stress on the cell can cause the unfolded protein response (UPR) pathway initiated by the cell in order to restore homeostasis. This pathway can activate caspase -12 which in turn can activate caspase-3 leading to programmed cell death of the nervous system in INCL patients (23).

DROSOPHILA MELANOGASTER AS A MODEL ORGANISM

The model organism used in this research project was *Drosophila melanogaster*. It is useful and effective for examining neurodegenerative diseases due to its short life span, easy maintainability, sequenced genome, complex brain and involved nervous system (7). Over 100 years of research has been conducted with the fruit fly and researchers have discovered over 70% of the genetic loci for human diseases have a conserved ortholog in *Drosophila*. Therefore, the fruit fly is a very useful model organism for the investigation of human diseases, such as Batten Disease (8).

Drosophila express a PPT1-like gene, called Ppt1, that is 55% identical and 72% similar to that seen in humans. The sequence alignment of fly Ppt1 alongside human

PPT1 can be seen in Figure 2. The black areas are where the alignments are identical and the white is where they are different (8).

QuickTime™ and a
TIFF (LZW) decompressor
are needed to see this picture.

Figure 3: A sequence alignment of human, bovine, mouse and fly Ppt1 (8).

Ppt1 is also functionally identical in that it cleaves the same substrate as its human ortholog. It is also identical at the biochemical level seeing as the *Drosophila* form of Ppt1 contains the conserved serine-aspartate-histidine catalytic triad necessary for enzymatic activity. This catalytic triad is a structurally identical active site shared between Ppt1 and PPT1 (see Figure 3) (1). These similarities make it possible to accurately model INCL within *Drosophila*.

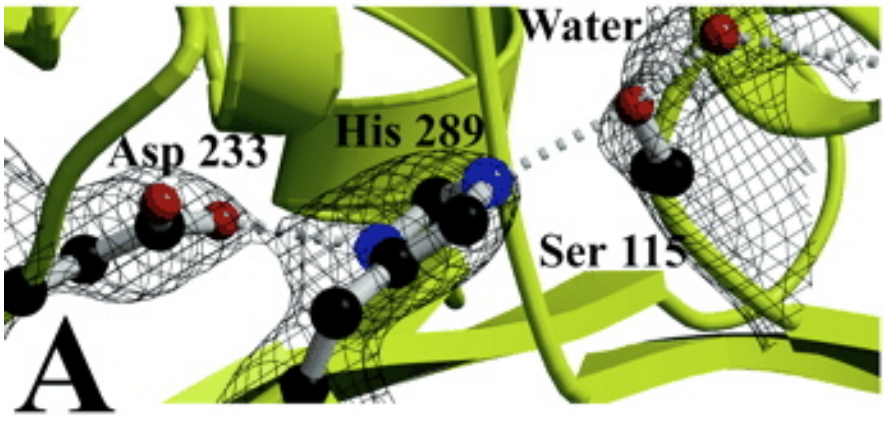

Figure 4: The conserved serine-aspartate-histidine catalytic triad (1).

Previous researchers have investigated many different mutations in order to model INCL in *Drosophila*, the first of which being the deletion of the gene coding for Ppt1 and three neighboring genes. Unfortunately, model organisms are typically unable to model disease flawlessly. This is true for *Drosophila* as well, however, Ppt1 deficient flies do exhibit the accumulation of autofluorescent storage materials (3). This material seems to differ in composition to the human GRODs and were actually more similar in biochemical make-up to the build-up found in human Tay-Sachs and Sandhoff diseases, two other lysosomal storage disorders (12). In addition, flies lacking Ppt1 do not experience neurodegeneration, but have a shorter lifespan than wild type flies (3).

There has been less research done on Ppt2, but the fly ortholog is 40% identical and 57% similar to the PPT2 gene seen in humans. Additionally, PPT2 shares a 26% identity with PPT1 and as said before, they have an 18% amino acid homology. A similar conserved catalytic triad in PPT1 is also seen in PPT2, which accounts for its similarity in function (see Figure 4) (2).

Figure 5: An electron density map of the PPT2 conserved serine-aspartate-histidine catalytic triad using crystallography-NMR software (2).

Unfortunately, the crystal structures of *Drosophila* Ppt1 and Ppt2 have not been thoroughly compared to the human forms. Therefore, there is a need to investigate the possible similarities in order to ensure that it would be possible to model the disorder if flies.

RNA INTERFERENCE IN THIS INVESTIGATION

In previous research studies on Ppt1 with *Drosophila*, researchers have investigated the effects of gene knock-out of Ppt1 and single point mutations of Ppt1. Gene knock-out involves the removal of an entire portion of DNA from the *Drosophila* genome, which prevents the production of any Ppt1 protein. The disadvantage in modeling the disease in this manner is the impossibility to remove solely the portion of DNA coding for Ppt1 and therefore other genes were silenced as well. A single point mutation entails the alteration of a single nucleotide within the segment of DNA that encodes Ppt1. This mutation did not completely silence Ppt1 gene expression, but produced a less effective form of Ppt1 (3).

In terms of Ppt2, investigators have looked at the phenotype of Ppt2 knock out in mice, but this has never before been performed in *Drosophila*. While the disease characteristics of the PPT2 knock-out mice were not as severe as the PPT1 knock-out mice, the presence of autofluorescent storage material was still present. The researchers in this study concluded, however, that PPT2 must serve a separate role as PPT1 (10). In terms of *Drosophila* research, there remains a large amount of ground to be covered both in terms of knock-out and knock-down with PPT2.

In this research project, the effects of gene knock-down of Ppt1 and Ppt2 using RNA interference (RNAi) was investigated. RNAi is a technique for halting mRNA from

making proteins and is 75% to 90% effective for the Ppt1 gene in *Drosophila*. It is superior to the two aforementioned techniques because it can more accurately hinder Ppt1 and Ppt2 expression. Furthermore, this knock-down can be achieved in a tissue-specific manner allowing researchers to specifically target a tissue. In the present study, RNAi was conducted specifically in neural tissues and therefore, all other cell types had both Ppt1 and Ppt2 present (19).

RNAi involves the production of a long double stranded RNA (dsRNA) that travels into the cytoplasm of cells. A protein complex, called Dicer, recognizes dsRNA and degrades it into small interfering RNA (siRNA) about 20 nucleotides long. One of the two strands of the siRNA is the guide strand complementary to the mRNA coding for Ppt1.The other strand is the passenger strand. Argonaute, a complex of catalytic proteins, binds to siRNA forming what is referred to as the RNA-induced silencing complex (RISC). RISC cleaves off the passenger strand from the dsRNA, binds to the complement target mRNA coding for Ppt1 or Ppt2 and degrades it, ultimately hindering Ppt1 or Ppt2 production (19).

GAL4-UAS SYSTEM

In order to initiate RNAi, a gene within the fly genome needed to be activated that produced a dsRNA containing segments complementary to the Ppt1 and Ppt2 mRNA. This gene was activated using the GAL4-UAS system in which two transgenic fly lines were designed and utilized. The first line is the UAS-Ppt1 transgene fly, in which the transgene coding for the Ppt1 or Ppt2 dsRNA is placed downstream of a UAS activation domain that consists of GAL4 binding sites. GAL4 is essentially an activator, the absence of GAL4 renders the transgene coding for dsRNA inactive in the UAS-Ppt1 and UAS-

Ppt2 flies. In order to activate the gene, the UAS-Ppt1 and UAS-Ppt2 flies were crossed with Enhancer-trap GAL4 flies. Therefore, the progeny of the cross expressed the target transgene encoding the dsRNA necessary for RNAi (see Figure 6) (6).

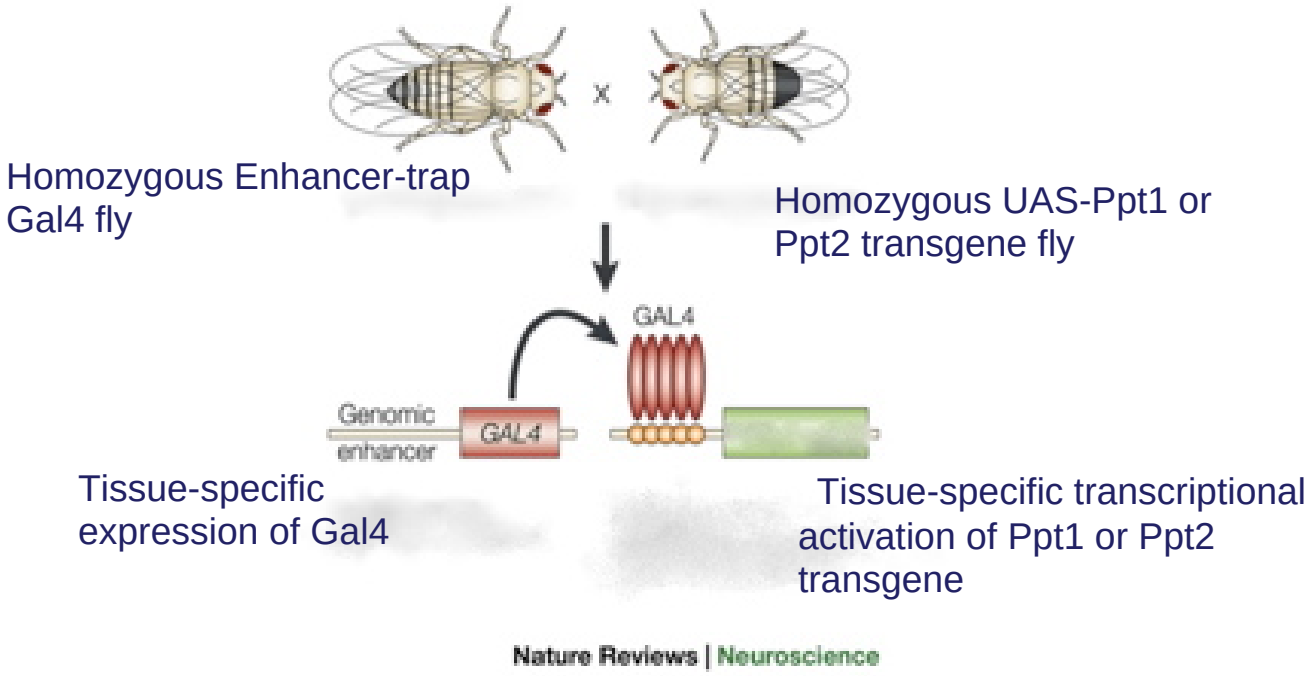

Figure 6: Illustration of the UAS-Gal4 system with labelled parent flies as well as a depiction of the effects of how the RNAi transgene for either Ppt1 or Ppt2 is activated in the progeny (18).

AIM OF INVESTIGATION

The purpose of this study was to investigate whether or not Ppt1 and Ppt2 RNAi knock-down had an effect during *Drosophila* neural development and on larval motor ability. First, a bioinformatics study was completed in order to investigate structural similarities between human PPT1, human PPT2, *Drosophila* Ppt1 and *Drosophila* Ppt2. This examination involved the compilation of PPT1 and PPT2 published crystal

structures as well as FASTA amino acid sequences for all four proteins. These sequences were then threaded into the crystal structures using the computer program DeepView / Swiss-pdb Viewer (4). This allowed us to visualize the structural similarities between the fly and human versions of these genes to further support our evaluation of PPT1 and PPT2 as having a useful ortholog in flies and it potentially playing a role in INCL.

The following fly crosses were used to investigate the effects of Ppt1 RNAi induced knock-down on CNS development: 5499x8760, 25952x8760, 5499x7470, and 5499x7466. 5499 and 25952 are UAS-Ppt1 transgene flies while 8760, 7470 and 7466 are the Enhancer-trap Gal4 flies. For Ppt2 RNAi induced knock-down, the crosses used are as follows: 1458x8760, 1459x8760. 1459 and 1458 are UAS-Ppt2 transgene flies and again, 8760 carried the Enhancer-trap GAL4 information. The fly crosses were created using female virgin flies from one strain and male flies from the other. Embryos of the F1 generation were collected, stained with FasII and examined with a SPOT color CCD camera.

Each stage 16 well-stained embryo was observed and compared to wild type embryos at stage 16. Furthermore, as an extra control, embryos were compared to those collected from each parent fly strain. In this investigation, the main component viewed was the central nervous system. Fas II staining of the central nervous system is expressed in three discrete subsets of axons that run the entire length of the embryo during late neurogenesis as seen in Figure 4 (3). Abnormal embryos were identified by discontinuities, disorganization, or scalloped appearance in these three subsets of axons. After the embryos were observed, the numbers of abnormal embryos and normal embryos were tallied and percentages were calculated for each cross. Abnormal embryos for Ppt1 deficiency were also classified into four groups based on severity: extremely

mild, mild, severe, and extremely severe. The various effects of RNAi from specimen to specimen determined this degree of severity.

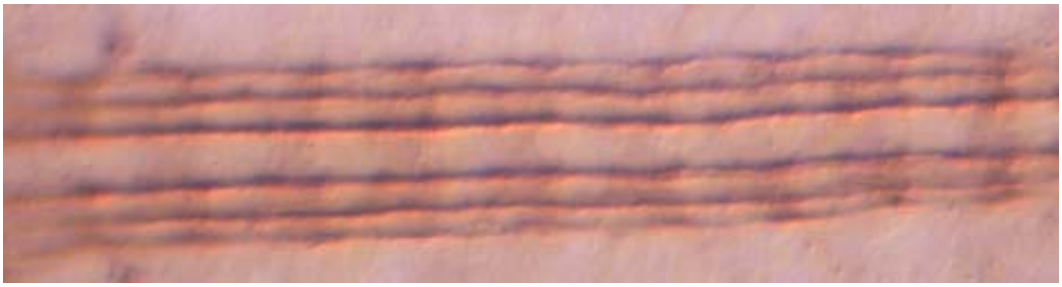

Figure 7: A *Drosophila* wild type central nervous system as visualized by a FasII staining.

Beyond staining embryos, motor ability of mutant larvae was evaluated in order to further correlate the fly phenotype to the human phenotype. As stated before, motor problems are seen in humans and motor differences in Ppt1 or Ppt2 knock-down larvae would further support that these flies are successful model organisms for this experiment. In order to access motor ability, mutant and wild type larvae were subjected to two motor assessments. The techniques in this study have been used previously by researchers to investigate the behavioral locomotion in *Drosophila* larvae carrying the yellow gene. This gene causes pigmentation and locomotion problems in *Drosophila* (14). The technique involves watching larvae transverse across an agar plate, while keeping track of how far they travel in a two minute period and how many lateral bending motions they make during this period. These locomotor characteristics tell us how many turns the larvae made (lateral bending) and how fast the larvae are able to move (distance traveled).

EXPERIMENTAL METHODS

PROTOCOL FOR BIOINFORMATICS IN DEEPVIEWER / SWISS PDB (4)

Crystal structure data for PPT1 and PPT2 from PDB.org was downloaded in a pdb.txt format. The FASTA amino acid sequences were then found and downloaded for PPT1, PPT2, Ppt1 and Ppt2 from uni-prot.org. The crystal structure for both PPT1 and PPT2 was opened in Deepviewer and various protein FASTA sequences were threaded through the crystal structures:

1. Ppt1 (Pubmed #Q9W3C7)was threaded through PPT1 (PDB #3GRO)
2. Ppt2 (Pubmed #Q9VKH6) was threaded through PPT2 (PDB #3PJA)
3. PPT2 (Pubmed #Q9UMR5) was threaded through PPT1 (PDB #3GRO)

The threading was completed using the following program within the Swiss PDB program:

1) Choose **Alignment** from the **Windows** tab in the toolbar at the top
2) A separate window should appear. Click on the very first line that indicates the pKa of the molecule. It should turn red.
3) In the **Fit** toolbar at the top, choose **Magic Fit**. After this is done, choose **Improved Fit** from the same toolbar. This will optimize the alignment.
4) In the **Color** toolbar, choose **Color By Alignment Diversity**.
5) In the **Swiss Model** toobar choose **Update Threading Now**, unless **Update Threading Display Automatically** is already chosen.
6) Click on the little arrow located to the right of the question mark of the alignment window. The window should expand and show a curve that shows the energy of the residue. The residue is stable when it's energy is below zero.

7) Click on the **Smooth** text in the window and change the smoothing factor to 1. This means that the energy of each residue will be the average of the energy itself and the energy of 1 flanking residue on each side.
8) In the **Swiss Model** toolbar, choose **Auto Color By Threading Energy** to better visualize the potential energy of each structure.
9) Click on the E=XX text in the alignment window to re-compute the energy for the model.
10) Click the **Select** toolbar, choose **Residues Making Clashes** to stabilize the model. This can be done multiple times to adjust the model.

EMBRYO COLLECTION, STAINING, AND IMAGING

Fly strains were kept at a constant temperature of 25°C with standard fly food (recipe below). The fly strains came from the Vienna Fly Stock Center and included 5499, 25952, 7470, 7466, 8760, 1458 and 1459. Flies from each individual mutant strain were transferred to collection bottles with molasses/yeast caps (recipe below). The female flies laid their embryos on the molasses/yeast caps overnight. Every 24 hours, these plates were changed and embryos were washed off onto a filter. The filter along with the embryos was placed into bleach for five minutes. All embryos were then placed in a 1.5mL microfuge tube with 500 uL FIX solution (450uL PEM and 50uL 37% formaldehyde) and 500uL heptane for 20min at room temperature. During this time, the microfuge tubes were agitated vigorously on the vortex to remove the vitelline membranes. The FIX solution was removed and the embryos were placed in methanol and agitated for 30 seconds to separate the interphase material. The heptane, methanol, and material in interphase were removed leaving only the devitellinized embryos at the

bottom of the microfuge tube. The embryos were then washed three times in methanol and preserved at -20'C.

Fly Food
12 g agar
44 g yeast
105 g cornmeal
700 mL H_20
Boil for 10 minutes
Add 750 mL H_20
Cool to 65°C
Add 10 mL 30% Tegosept and 10 mL propinoic acid
Mix for 5 minutes, pour into containers, cap containers once food is hardened
Store food in the 4°C

Molasses plates
4 g agar
6 mL molasses
100 mL H_20
Microwave until agar dissolves
Pour into Petri dish caps, allow to harden
Store in 4°C

50uL of embryos stored in methanol at 20'C were re-hydrated in 0.1% PBT (500mL Phosphate buffered saline solution and 1mL Triton X-100) in a 1.5mL microfuge tube. Embryos were washed in 1mL PBT for 30min, rocking at room temperature. Diluted Normal Goat Serum (NGS) (1mL PBT and 50 uL NGS) was then added to the embryos for 30 minutes, rocking at room temperature. The primary antibody, FAS II, was diluted at 1:5 (75uL antibody and 375uL PBT) and added to the embryos. The embryos were then incubated, rocking overnight at 4'C.

The next day, the primary antibody was removed and embryos were rinsed 3 times in PBT. The embryos were washed for 1 hour in PBT, changing solutions every 15 minutes. The secondary antibody (GαM-HRP) was diluted at 1:250 using PBT. The secondary antibody was added to the samples and incubated for 1 hour at room

temperature. The secondary antibody was removed and the samples were rinsed 3 times in PBT. The tissues were washed for 1 hour in PBT, changing solutions every 30 minutes. After the final wash, all PBT was removed and 300uL premade DAB and 30uL hydrogen peroxide (diluted previously to 1:100) was added. The reaction was observed under a microscope and it continued until the embryos turned dark brown. Washing the embryos with PBT 3 times then stopped the reaction. The embryos were then dehydrated by adding 1 mL 50% ethanol for 5 minutes, then 1mL 70% ethanol for five minutes and finally 1 mL 100% ethanol overnight.

The next day, the ethanol was removed and 700uL of methyl salicylate was added. The samples were either stored at 4'C or mounted on slides to view under the microscope. All samples and slides were stored at 4'C and in the dark.

FLY CROSSES

Ppt1 RNAi induced knock-down crosses:

~ 5499 (Vienna Drosophila RNAi Center: 44Dd/CyO) crossed with 8760 (Bloomington Drosophila Stock Center: Gal4-ELAV)
~ 5499 (Vienna Drosophila RNAi Center: 44Dd/CyO) crossed with 7466 (Bloomington Drosophila Stock Center: CQ2-GAL4)
~ 5499 (Vienna Drosophila RNAi Center: 44Dd/CyO) crossed with 7470 (Bloomington Drosophila Stock Center: RN2-GAL4)
~ 25952 (Vienna Drosophila RNAi Center: TRIP.JF01972) crossed with 8760 (Bloomington Drosophila Stock Center: Gal4-ELAV)

Ppt2 RNAi induced knock-down crosses:

~ 1458 (Vienna Drosophila RNAi Center: w1118; P{GD399}v1458/TM3) crossed with 8760 (Bloomington Drosophila Stock Center: Gal4-ELAV)
~ 1459 (Vienna Drosophila RNAi Center: P{neoFRT}82B P{πM}87E P{πM}97E) crossed with 8760 (Bloomington Drosophila Stock Center: Gal4-ELAV)

ASSESSMENT OF LARVAE LOCOMOTION

Females flies from both the 5499x8760 (Ppt1 RNAi) cross and 2376 (wild type) were allowed to oviposit for 24 hours on molasses plates. Behaviors were then scored in larvae aged 48, 72, 96, and 120 hours post-hatching.

Larval locomotor activity was documented through the use of clear shallow rectangular plastic boxes 17 cm in length, 14 cm in width and 2 cm in height filled to a depth of 1 cm with 1.5% agar-gel. A grid of 1 cm by 1 cm squares was attached to the underside of the box so that it could be viewed from above through the agar and plastic. Ppt1 RNAi knock-down flies and wild type flies were transferred individually onto the center of the agar surface and the path of each larvae was monitored using an Olympus SZ40 stereozoom microscope for two minutes each. The total number of squares crossed during this period was recorded. Furthermore, lateral bending of the head and anterior segment was also scored for 2 minutes. The amount of larvae tested for both locomotor characteristics was 25.

RESULTS/DISCUSSION

The bioinformatics investigation took a look at three different investigations of threading FASTA sequences into crystal structures. First, the *Drosophila* Ppt1 FASTA amino acid sequence was threaded into the human PPT1 crystal structure. This showed considerable similarities between the two proteins as indicated by the blue areas of Figure 13 where the threading was most stable given molecular forces such as Van Der Waals forces, hydrophobic interactions, and hydrogen bonding. Next, the *Drosophila* Ppt2 FASTA sequence was threaded into the human PPT2 crystal structure. Again, areas of the most stabilization are shown in blue, while other colors show differing areas less stability with red being the least stable. Finally, the human PPT2 FASTA sequence was threaded into the human PPT1 crystal structure showing large areas of structural similarity.

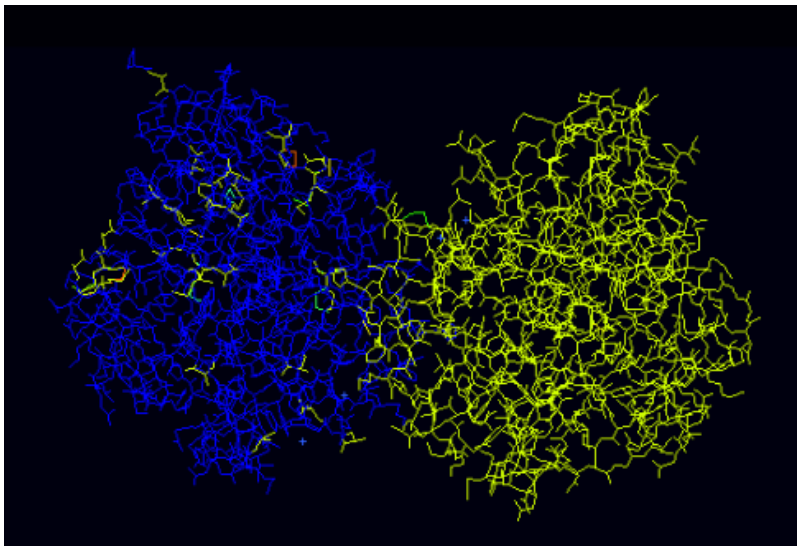

Figure 8: *Drosophila* Ppt1 FASTA information threaded into the PPT1 Human crystal structure.

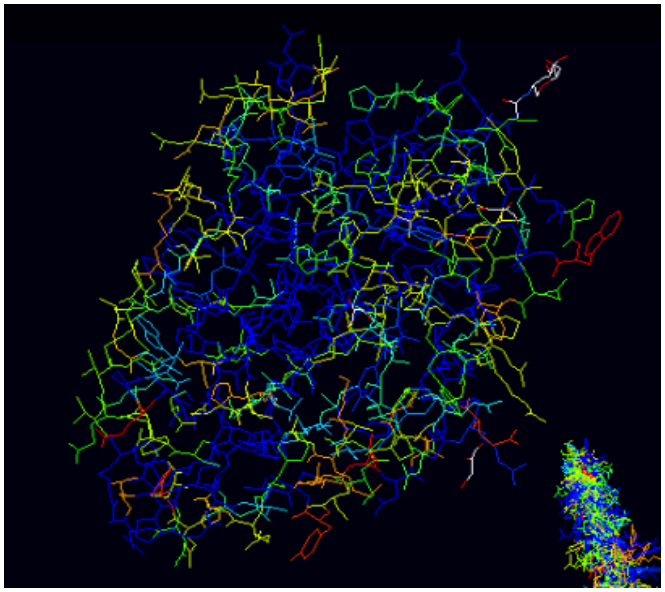

Figure 9: *Drosophila* Ppt2 FASTA information threaded into the human PPT2 crystal structure.

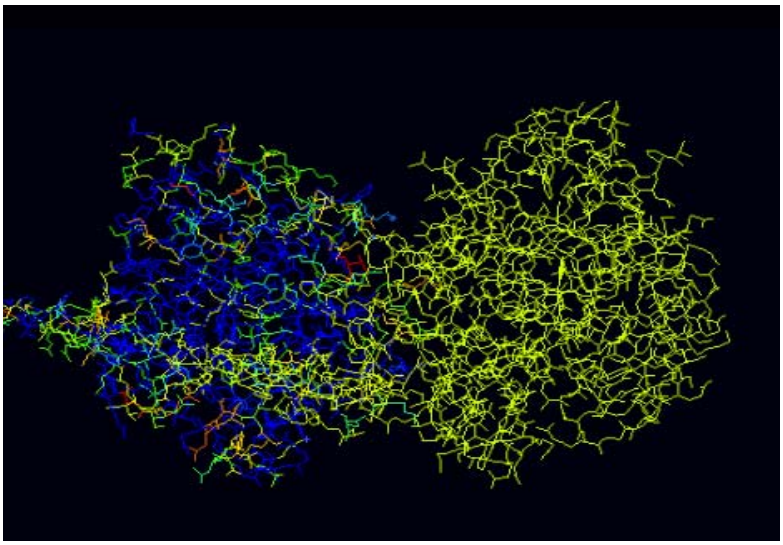

Figure 10: Human PPT2 FASTA sequence threaded into the human PPT1 crystal structure.

IMAGES AND ANALYSIS OF *DROSOPHILA* EMBRYONIC NEUROGENESIS

Images of embryos from each cross were taken and saved. All were stage 16 embryos and stained with FAS II, which is expressed in three discrete axon bundles that extend longitudinally down either side of the ventral midline of the embryo. Each cross achieved the same purpose, which was to produce the dsRNA required for RNAi of Ppt1

production specifically in neural tissue. Thus, they all exhibited the same types of phenotypes in the central nervous system, which included discontinuities, thinned and thickened axon bundles, and disorganized subsets of axons as seen in the following figures. Example of both a wild type and an abnormal central nervous system can be seen below in Figures 11 and 12, respectively.

Figure 11: Wild Type embryo stained with FasII.

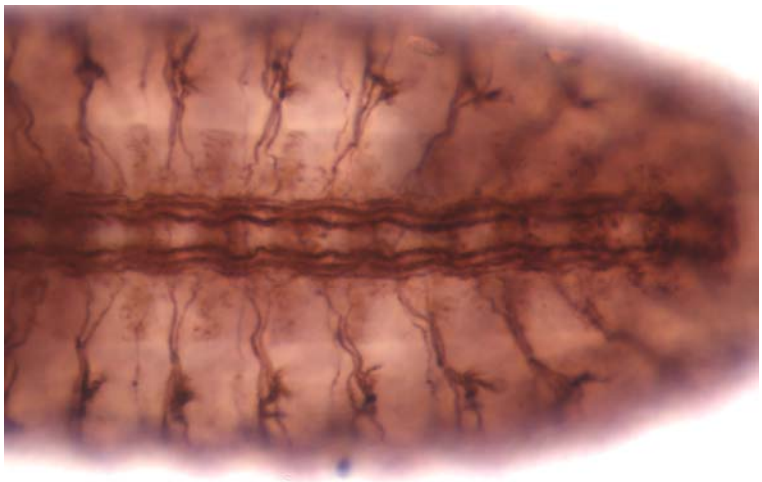

Figure 12: Abnormal RNAi embryo from 5499 x 8760 cross

Table 1 summarizes the embryo analysis data from each cross. It can be seen in this table that each cross exhibited a large number of abnormalities as was expected. The normal embryos could have occurred due to contamination within the crosses or could have exhibited a phenotype so mild that it was unnoticeably different from wild type. This data demonstrates, however, that Ppt1 RNAi knock-down does have an effect during neural development.

Fly Strain	**# of embryos at s16**	**# w/ abnormalities**	**% w/ abnormalities**
5499 x 8760	81	81	100
5499 x 7466	67	57	85
5499 x 7470	106	99	93.4
25952 x 8760	42	36	85.7

Table 2: Summary of embryo analysis from each cross.

Figure 13 shows an example of the type of analysis underwent by each embryo cross. Not only were embryos in the crosses from Table 2 compared to wild type embryos, but they were also compared to embryos from each individual parent strain as a control. In Table 3 below, the control data from investigating the progeny of each

individual strain supports the assertion that the development of the central nervous system was disrupted by RNAi induced knock down of Ppt1.

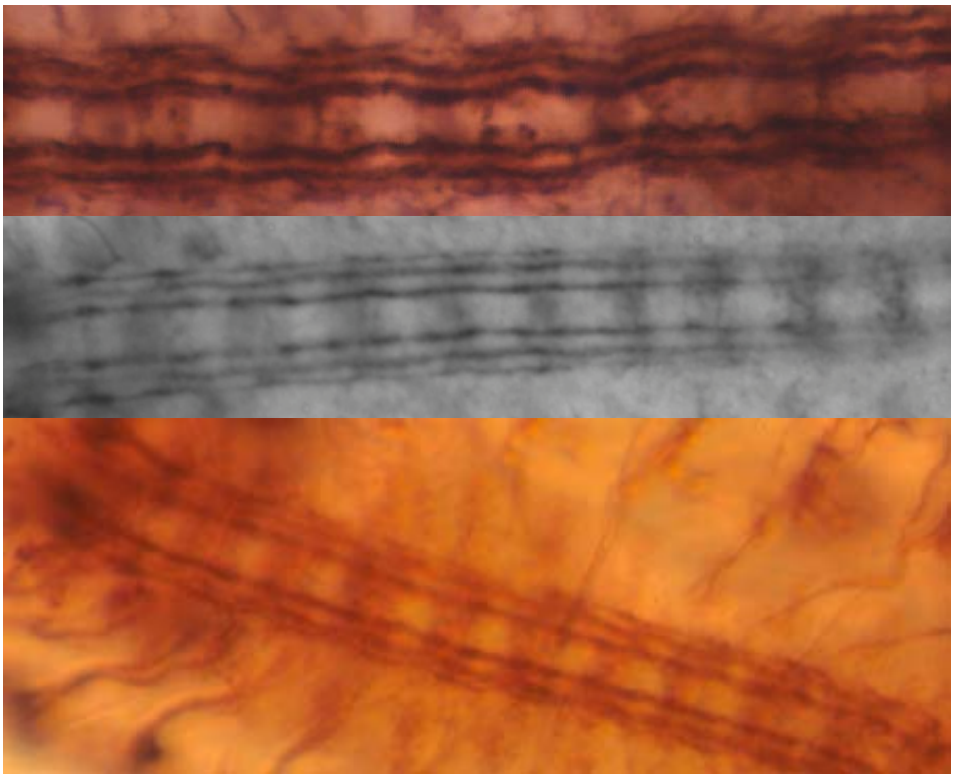

Figure 13: Top image is CNS of 5499x8760 progeny. The middle image is of a 8760 only progeny and the bottom image is of a 5499 only progeny.

Genotype	% Deefective
$Ppt1^{5499}$RNAi	0.03 (30)
$Ppt1^{25952}$RNAi	0 (30)
Elav-gal4 (8760)	0 (33)
UAS tauLacZ CQ2-gal4 (7466)	0 (30)
UAS tauLacZ RN2-gal4 (7470)	0 (35)

Table 3: Percentage of defective embryos for each parent strain in the Gal4-UAS system. Parentheses represent the number of embryos assayed.

An interesting aspect of this data is that a spectrum of severity can be seen ranging from extremely mild to extremely severe as seen in Figure 14. This is most likely due to the fact that the RNAi technology used to knock-down Ppt1 is 70% - 90% effective.

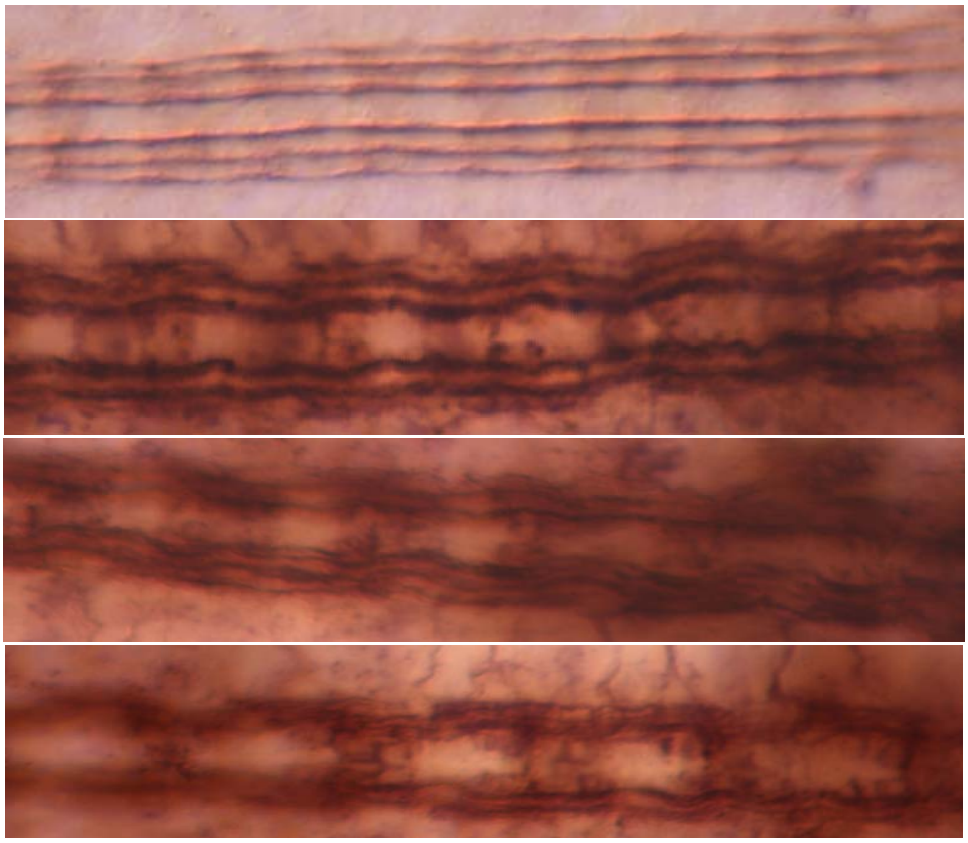

Figure 14: The RNAi spectrum of severity. Ranging from wild type at the top to one of the most severely abnormal phenotypes at the bottom.

Table 4 summarizes the severity of defects seen in the abnormal embryos of each cross. Stage 16 embryos were categorized into four different groups: extremely mild, mild, severe, and extremely severe. The classification was based on perceived severity as seen in Figures 15-18.

It can also be seen that the 5499 x 7470 cross exhibited the most severe phenotype which suggests that this cross expresses the most effective form of the UAS-Ppt1

transgene as activated by Gal4. This could also mean that this cross is the most effective at modeling INCL as it seems to knock-down a larger percentage of Ppt1.

Fly Strain	**% extremely mild abnormalities**	**% mild abnormalities**	**% severe abnormalities**	**% extremely severe abnormalities**
5499 x 8760	2.5	47	43	7.4
5499 x 7466	6	31	42	10.4
5499 x 7470	4.7	33	50.9	9.4
25952 x 8760	16.6	42.8	31	2.3

Table 4: Summary of severity of abnormalities seen in the abnormal embryos of each cross.

Figure 15: Extremely Mild abnormal embryo from cross 5499 x 7466

Figure 16: Mild abnormal embryo from cross 5499 x 7466

Figure 17: Severe abnormal embryo from cross 5499 x 7466

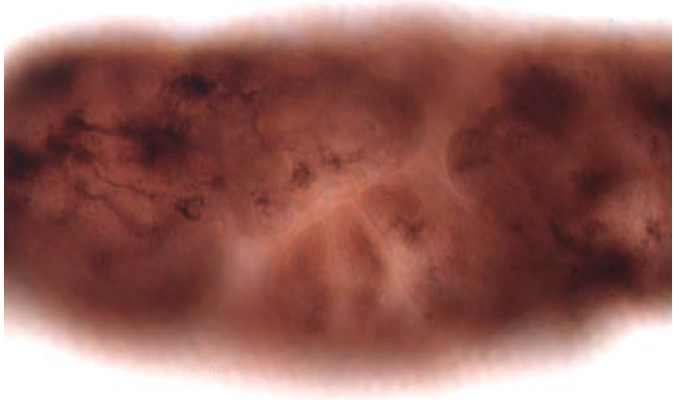

Figure 18: Extremely severe abnormal embryo from cross 5499 x 7466

Figure 12 shows the abnormal phenotype seen for Ppt2 RNAi knock-down embryos. These embryos were also stage 16 and underwent the same protocol as the Ppt1 knock-down embryos. Furthermore, they exhibited a very similar phenotype with faulty axonal pathfinding in the PNS, disorganized and discontinuous axons in the CNS and abnormally thick and thin sections of the CNS (3).

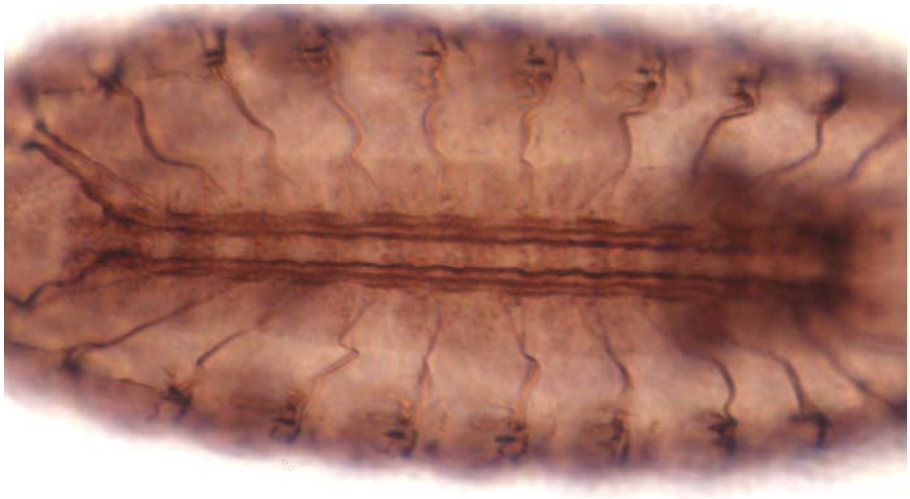

Figure 19: Abnormal Ppt2 RNAi knock down embryo from 1459x8760 stained with FAS II antibody.

Table 5 summarizes the embryo analysis data from each cross for the Ppt2 induced knock-down strains. It can be seen in this table that each cross exhibited abnormalities very similar to those seen in Ppt1 RNAi knock down. Again, the normal embryos could have occurred due to contamination within the crosses or could have exhibited a phenotype so mild that it was unnoticeably different from wild type. This data shows, however, that Ppt2 RNAi knock-down has an effect during embryonic neurogenesis in *Drosophila*. Unfortunately, the embryos from the parent strains are yet

to be evaluated and therefore, only the Elav-Gal4 embryo information from the previous experiment with Ppt1 was able to act as a control for the data. (see Figure 20).

The presence of a phenotype illustrates that Ppt2 is involved in the development of the CNS and the lack of this gene results in CNS disruption. Furthermore, the observable phenotype seemed to be less severe than Ppt1 RNAi induced knock-down indicating that Ppt1 may be more important during CNS development than Ppt2.

Fly Strain	**# of embryos at s16**	**# w/ abnormalities**	**% w/ abnormalities**
1459 x 8760	35	32	91.4
1458 x 7466	10	7	100

Table 5: Summary of embryo analysis from each Ppt2 knock-down cross.

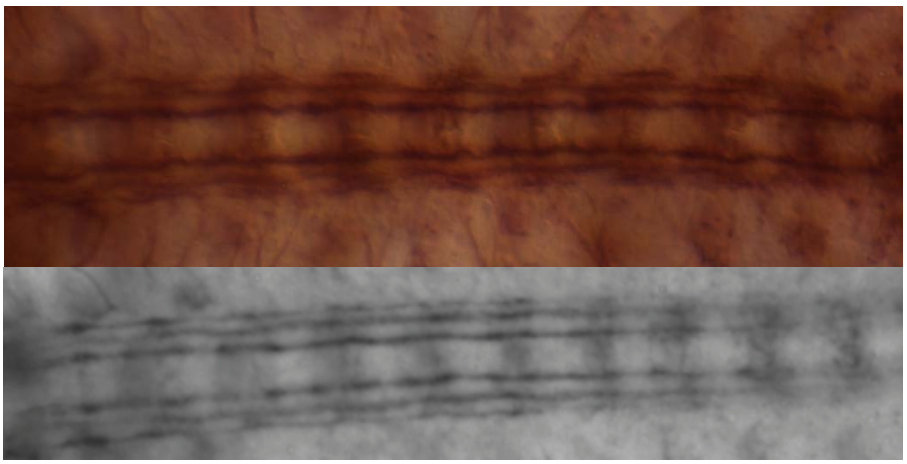

Figure 20: Top image is that of a 1459x8760 CNS. The bottom image is the CNS of 8760 progeny.

LOCOMOTION DATA AND ANALYSIS

Figure 21 shows locomotor activity of larvae of the Ppt1 RNAi induced knock-down strain and wild type strain. Larval locomotion is developmentally related and therefore, there are differing amounts of lateral bending for different stages of larval development (14). Lateral bending occurrences were similar during 72h or 96h of development between the two strains. At 48h and 120h, however, there seemed to be significant differences in lateral bending movements where wild type larvae had more lateral bending events. Each lateral bend is followed by a change in direction. Thus, it can be concluded that at 48h and 120h of development, the Ppt1 knock-down larvae are moving in a straighter path as opposed to the wild type larvae which are making more turns.

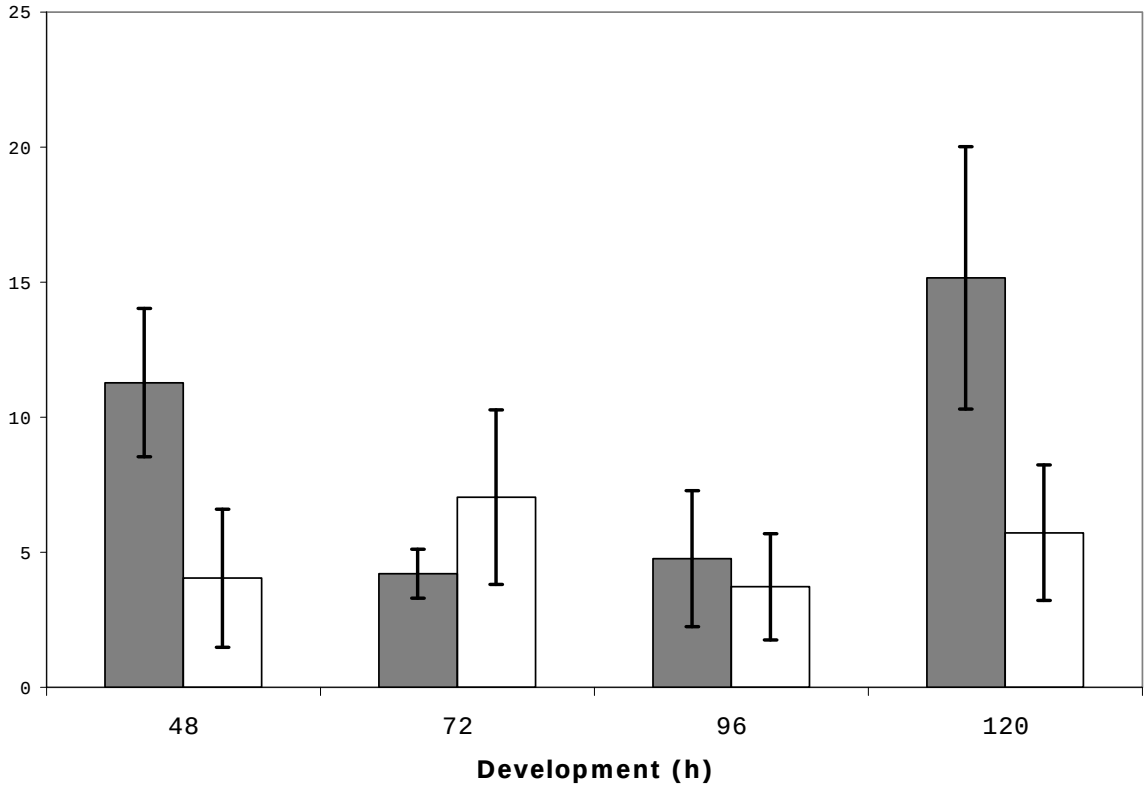

Figure 21: Bending behavior for both wild type and Ppt1 knock-down larvae at various ages within a 2 minute period. White represents the mutant, while grey indicated the wild type strain.

Similarly, the locomotion data that accounted for how far larvae of each strain traveled in a two minute period showed that there is not much difference at some stages. During the 72h period of development, there was a significant difference in locomotion with the mutant strain traveling farther than wild type. Overall, wild type on average transversed a shorter distance than Ppt1 knock-down flies.

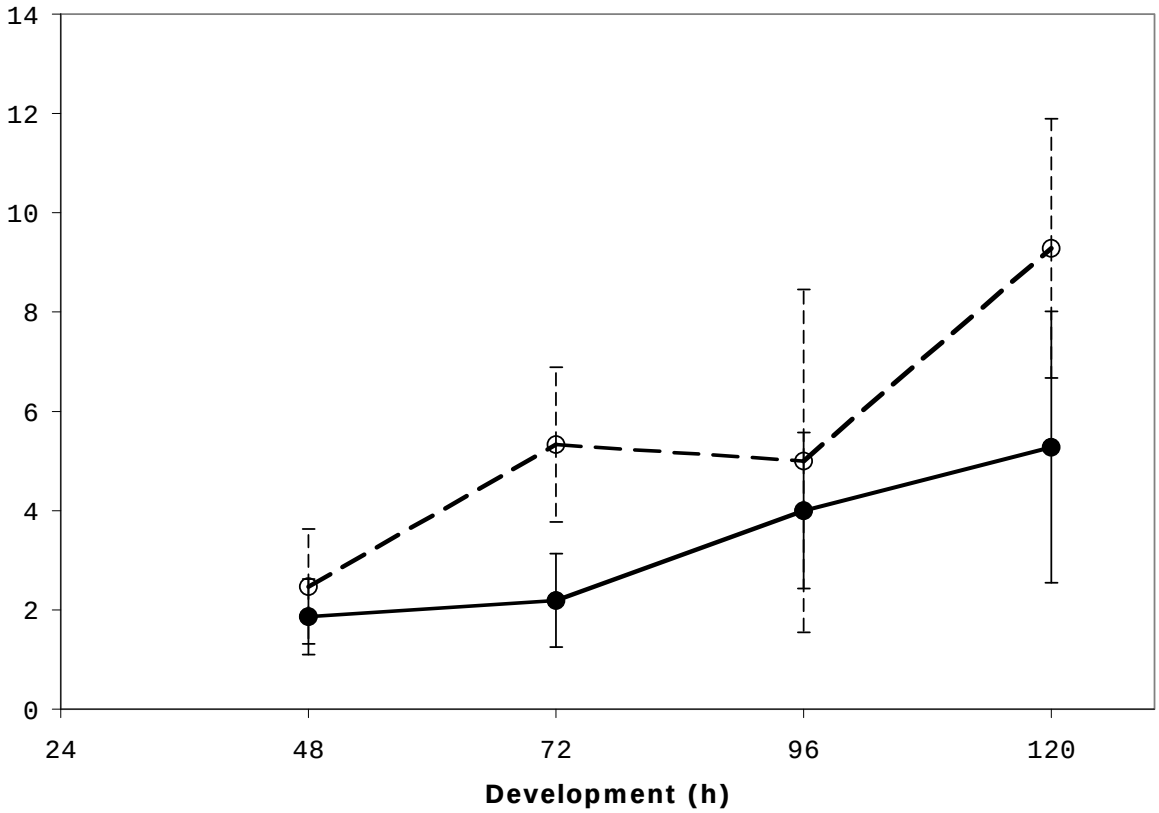

Figure 22: Locomotor activity of wild type and Ppt1 knock-down flies at various ages. White represents the mutant strain and black indicated the wild type strain. Larval locomotion was measured as a number of squares crossed in two minutes.

As far as drawing conclusions from these two figures, it is difficult to make any definitive deductions regarding exactly how the two strains are different, but it can be noted that there is an abnormality present in the mutant strain that effects normal locomotion. Furthermore, error bars in these two figures were very large compared to

previous research with comparable sample sizes. This is most likely due to the larvae being born with a 24h collection period from female parent flies. This means that at what we perceived to be the 48hr period, there would be larvae that were considerably older. The error bars for the mutant strain was noticeably larger than the wild type in Figure 22 for three of four periods of development, which may be reflective of the ranging severity witnessed during the investigation of stained Ppt1 knock-down embryos. Since the data points have such variability, it is clear that modifications to the experimental method should be made in order to get clearer results.

CONCLUSIONS

The bioinformatics analysis in the study showed that Ppt1, Ppt2, PPT1, and PPT2 are structurally similar. This supports previous research that identifies Ppt1 and PPT1 as functionally identical and that PPT2 performs a similar function to PPT1 (10). Furthermore, the embryonic study in this experiment showed that Ppt1 induced knock-down results in an abnormal phenotype, which indicates that Ppt1 plays a role in embryonic neurogenesis. Similarly, Ppt2 knock-down resulted in a similar phenotype and therefore, it may be concluded that it also plays a role in the process of neurogensis. These proteins, previously not regarded as developmentally significant, have been shown to be important during embryogenesis. In correlation with the human disorder, one may deduce that this data provides evidence that INCL patients could exhibit neurological pathology in utero.

Ppt2 has yet to be investigated on a functional level as compared to PPT2, however, their structural similarities suggest that they may be similar in function. Furthermore, the FAS II staining procedure in this experiment showed that there are likely similarities in function between Ppt1 and Ppt2 since they resulted in the same phenotype. Since it is know that Ppt1 and PPT1 perform the same function, Ppt2 and PPT2 are structurally similar, and that the phenotype of Ppt1 knock-down and Ppt2 knock-down is very similar, it may be concluded that PPT2 may also play a role in INCL.

In terms of the locomotor evaluation, this study shows that the defects seen during embryogenesis may result in motor differences. While it remains to be identified whether or not these differences are defects in motor ability, there seems to be an abnormal motor phenotype in Ppt1 knock-down larvae. As was said before, the data points have large standard errors, but this may reflect the range of effects Ppt1 knock-down had on

embryos. It could be argued that these differences are not significant since the mutant strain did not have significant differences at all developmental stages, but synaptic plasticity may have accounted for some compensatory mechanism for movement. Furthermore, it could be possible that mutants with severe larval defects never progressed to a larval stage and thus, the only larvae experimented with in this study were those with more mild neural abnormalities.

FUTURE WORK

This research is a preliminary investigation into RNAi knock-down of the Ppt1 and Ppt2 genes. Now that it has been established that there is a phenotype worth exploring, the next step will be to examine the use of different antibody staining markers to investigate how different parts of the central nervous system of these *Drosophila* embryos is affected by Ppt1 and Ppt2 RNAi knock-down. Furthermore, 1459 and 1458 embryos need to be collected in order to act as a control for the Ppt2 knock-down data in this experiment.

Another area of this research worth exploring is the verification of RNAi knock-down using Q-PCR and reverse transcriptase PCR. In this way, the amount of RNAi knock-down that is actually occurring in these crosses can be quantified. Additionally, the research of other genes besides Ppt1 might offer better understanding of how INCL functions. The examination of the gene Spinster, a potential Ppt1 interacting gene, might provide information about how Ppt1 works in tandem with other genes (22). Finally, the analysis of Ppt2 knock-down larvae in the locomotor tests in this experiment would shed light on the behavioral effects of Ppt2 knock-down.

REFERENCES

1. Bellizzi, J.J. III, Joanne Widom, Christopher Kemp, Jui-Yun Lu, Amit K. Das, Sandra L. Hofmann, and Jon Clardy (2000). The crystal structure of palmitoyl protein thioesterase 1 and the molecular basis of infantile neuronal ceroid lipofuscinosis. *PNAS* 97: 4573-4578.

2. Calero, Guillermo, Praveena Gupta, M. Cristina Nonato, Sagun Tandel, Edward R. Biehl, Sandra L. Hofmann, and Jon Clardy (2003). The crystal structure of palmitoyl protein thioesterase-2 (PPT2) reveals the basis of divergent substrate specificities of the two lysosomal thioesterases, PPT1 and PPT2. *The Journal of Biological Chemistry* 278(39): 37957-37964.

3. Chu-LaGraff, Quynh, Cassandra Blanchette, Patrick O'Hern, and Cassandra Denefrio (2010). The batten disease palmitoyl protein thioesterase 1 gene regulates neural specification and axon connectivity during *Drosophila* embryonic development. *PLoS One* 5(12): e14402.

4. Chu-LaGraff, Quynh (2010). Bioinformatics III: Analysis of human neurological diseases at the genetic level. Union College.

5. Dawson, G., and Cho, S. 2000. Batten Disease: Clues to Neuronal Protein Catabolism in Lysosomes. *Journal of Neuroscience Research* 60: 133-140.

6. Duffy J.B., and N. Perrimon (2002). The UAS/GAL4 system for tissue-specific analysis of EGFR gene function in *Drosophila melanogaster*. Key Experiments in Practical Developmental Biology. *Cambridge Univeristy Press* 20: 269-281.

7. Fortini, M.E., Skupski, M.P., Boguski, M.S., Hariharan, I.K. 2000. A survey of human disease gene counterparts in the *Drosophila* genome. *J. Cell Biology* 150: F23-F30

8. Glaser, R.L., Hickey, A.J., Chotkowski, H.L., Chu-LaGraff, Q. 2003. Characterization of *Drosophila* palmitoyl-protein thioesterase 1. *GENE* 312: 271-279.

9. Goebel, H.H., and Wisniewski, K. E. (2004). Current State of Clinical and Morphological Features in Human NCL. *Brain Pathology*. 14: 61-69.

10. Gupta, Praveena, Abigail A Soyombo, Armita Atashband, Krystyna E. Wisniewski, John M. Shelton, James A. Richardson, Robert E. Hammer, and Sandra L. Hofmann (2001). Disruption of PPT1 or PPT2 causes neuronal ceroid lipofuscinosis in knockout mice *PNAS* 98(24): 13566-13571.

11. Hellsten, Elina, Jouni Vesa, Vesa M. Olkkonen, Anu Jalanko, and Leena Peltonen (1996). Human palmitoyl protein thioesterase: evidence for lysosomal targeting of the enzyme and disturbed cellular routing in infantile neuronal ceroid lipofuscinosis. *The EMBO Journal* 14(19): 5240-5245.

12. Hickey, Anthony J., Heather L. Chotkowski, Navjot Singh, Jeffrey G. Ault, Christopher A. Korey, Marcy E. MacDonald, and Robert L. Glaser (2006). Genetics 172(4): 2379-2390.

13. Hofmann, S.L. (2001). 3 positional candidate gene cloning of CLN1. *Advances in Genetics* 45: 69.

14. Inestrosa, Nibaldo C., Claudio E. Sunkel, Jorge Arrigada, Jorge Garrido and Raul Godoy-Herrera (1996). Abnormal development of the locomotor activity in yellow larvae of *Drosophila*: a cuticular defect? *Genetica* 97: 205-210.

15. Lehtovirta, M., Aija Kyttala, Eeva-Liisa Eskelinen, Michael Hess, Outi Heinonen, and Anu Jalanko (2001). Palmitoyl protein thioesterase (PPT) localizes into synaptosomes and synaptic vesicles in neurons: implications for neuronal ceroid lipofuscinosis (INCL). *Human Molecular Genetics* 10: 69-75.

16. Mole, S.E. and M. Gardiner (1999). Molecular genetics of the neuronal ceroid lipofuscinosis. *Epilepsia* 40: 29-32.

17. Mole, S.E. (2004). The Genetic Spectrum of Human Neuronal Ceroid –lipofuscinosis. *Brain Pathology* 14: 70-76.

18. Muqit, Miratul M. K. and Mel B. Feany (2002). Modelling neurodegenerative diseases in *Drosophila*: a fruitful approach? Nature Reviews Neuroscience 3: 237-243.

19. "RNAi - Interference RNA." University of Miami Department of Biology. Web. 11 Aug. 2009 <http://www.bio.miami.edu/~cmallery/150/gene/siRNA.htm>.

20. Satishchandra P. and S. Sinha. Progressive myoclonic epilepsy. *Indian perspective* 58(4): 514-522.

21. Soyombo, Abigail A., and Sandra Hofmann (1997). Molecular cloning and expression of palmitoyl-protein thioesterase 2 (PPT2), a homolog of lysosomal palmitoyl-protein thioesterase with a distinct substrate specificity. *The Journal of Biological Chemistry* 272: 27456-27463.

22. Sweeney, Sean t. and Graeme W. Davis (2002). Unrestricted synaptic growth in spinster- a late endosomal protein implicated in TGF-β-mediated synaptic growth regulation. *Neuron* 36: 403-416.

23. Wei et al., (2008). ER and oxidative stresses are common mediators of apoptosis in both neurodegenerative and non-neurodegenerative lysosomal storage disorders and are alleviated by chemical chaperones. *Human Molecular Genetics* 17: 469-477.

OPEN ACCESS Freely available online

PLoS one

The Batten Disease *Palmitoyl Protein Thioesterase 1* Gene Regulates Neural Specification and Axon Connectivity during *Drosophila* Embryonic Development

Quynh Chu-LaGraff*, Cassandra Blanchette[¤a], Patrick O'Hern, Cassandra Denefrio[¤b]

Department of Biology, Union College, Schenectady, New York, United States of America

Abstract

Palmitoyl Protein Thioesterase 1 (PPT1) is an essential lysosomal protein in the mammalian nervous system whereby defects result in a fatal pediatric disease called Infantile Neuronal Ceroids Lipofuscinosis (INCL). Flies bearing mutations in the *Drosophila* ortholog *Ppt1* exhibit phenotypes similar to the human disease: accumulation of autofluorescence deposits and shortened adult lifespan. Since INCL patients die as young children, early developmental neural defects due to the loss of PPT1 are postulated but have yet to be elucidated. Here we show that *Drosophila Ppt1* is required during embryonic neural development. *Ppt1* embryos display numerous neural defects ranging from abnormal cell fate specification in a number of identified precursor lineages in the CNS, missing and disorganized neurons, faulty motoneuronal axon trajectory, and discontinuous, misaligned, and incorrect midline crossings of the longitudinal axon bundles of the ventral nerve cord. Defects in the PNS include a decreased number of sensory neurons, disorganized chordotonal neural clusters, and abnormally shaped neurons with aberrant dendritic projections. These results indicate that *Ppt1* is essential for proper neuronal cell fates and organization; and to establish the local environment for proper axon guidance and fasciculation. Ppt1 function is well conserved from humans to flies; thus the INCL pathologies may be due, in part, to the accumulation of various embryonic neural defects similar to that of *Drosophila*. These findings may be relevant for understanding the developmental origin of neural deficiencies in INCL.

Citation: Chu-LaGraff Q, Blanchette C, O'Hern P, Denefrio C (2010) The Batten Disease *Palmitoyl Protein Thioesterase 1* Gene Regulates Neural Specification and Axon Connectivity during *Drosophila* Embryonic Development. PLoS ONE 5(12): e14402. doi:10.1371/journal.pone.0014402

Editor: Michael N. Nitabach, Yale School of Medicine, United States of America

Received May 11, 2010; **Accepted** November 25, 2010; **Published** December 22, 2010

Funding: This work was supported by NIH-R15 NS046334, Merck-AAAS Undergraduate Fellowship, Booth-Ferris Fellowship, and Batten Disease Research and Support Association. The funders had no role in study design, data collection and analysis, decision to publish, or preparation of the manuscript.

Competing Interests: The authors have declared that no competing interests exist.

* E-mail: chulagrq@union.edu

¤a Current address: Neuroscience Program, University of Massachusetts Medical School-Worcester; Worcester, Massachusetts, United States of America
¤b Current address: Department of Neurobiology, Harvard Medical School, Boston, Massachusetts, United States of America

Introduction

Infantile Neuronal Ceroids Lipofuscinoses (INCL) belongs to a group of lysosomal storage disorders characterized by the fatal progressive deterioration of the visual and central nervous system, and the accumulation of abnormal autofluorescent storage materials in the brain [1,2]. INCL, the most severe form, results from defects in the protein Palmitoyl Protein Thioesterase 1 (PPT1) which encodes a lysosomal thioesterase that cleaves long fatty acids-most likely palmitate-attached to the cysteine residues of S-acylated protein substrates [3,4]. In mammals, PPT1 expression is found in all cell types at varying quantities with the highest levels in the brain, eye, and spleen [5,6]. In addition to being found in lysosomal compartments of neurons, the protein is also expressed in the pre-synaptic compartments [7,8,9].

Although ubiquitously expressed, PPT1 deficiency affects only the development and maintenance of cortical neurons in the nervous system. Afflicted children are normal at birth; but exhibit progressive cognitive and motor deficits, seizures, and ocular deterioration and eventual blindness by the age of 3; after which INCL children remain in a vegetative state until death in their teens. Microarray studies reveal that changes in gene expression can be detected at 10 week-old post-natal PPT1 knock-out mice brains, a time prior to neurodegenerative symptoms [10]. These findings suggest that the loss of this protein may have embryonic developmental consequences prior to being symptomatic. If PPT1 does have a role during embryonic neurogenesis, then the elucidation of the fundamental cellular pathways requiring PPT1 during development will be critical.

Using *Drosophila*, we investigate the role of PPT1 during the development of the embryonic nervous system. Previous studies indicated that the removal of the *Drosophila* ortholog *Ppt1* results in phenotypes similar to human INCL [11,12]. *Ppt1* loss-of-function (LOF) flies lacking Ppt1 enzymatic activity display some aspects of INCL disease: reduced life expectancy and an age-dependent accumulation of autofluorescent storage material in the adult CNS. Overexpression of Ppt1 in the larval visual system leads to increased cell death [13]. A dominant gain-of-function modifier screen for genes interacting with *Ppt1* suggests that it has a role in synaptic developmental pathways and the regulation of synaptic vesicle endocytosis [14].

Here, we investigate the potential role of *Ppt1* during the generation of the nervous system by focusing on discreet identified neuronal cell lineages. We hypothesize that while *Ppt1* mutants

may not show detectable adult brain abnormality, early defects at the cellular level may be present in the form of altered cell fate specification, proliferation, and axon guidance and connectivity. Our results support this hypothesis and indicate that the loss of *Ppt1* has consequences much earlier than previously described. *Ppt1* defects lead to mis-specification of identified CNS and PNS neural precursor cell fates, an abnormal complement of neural precursors and neurons, and motoneuronal axonal misrouting and overall defective axon pathfinding and fasciculation. These *Ppt1*-associated embryonic phenotypes may contribute to the shortened lifespan of *Ppt1*-deficient flies. These findings in *Drosophila* may be relevant in identifying the earliest developmental neural defects in INCL afflicted individuals and potential cellular targets for therapeutic interventions.

Results

Drosophila Ppt1 RNA and protein are expressed at very low/undetectable levels

To ascertain the endogenous RNA Ppt1 expression pattern during development, whole mount *in situ* experiments on various developmentally staged embryos (from 0 hr. to 16 hr), and wing, leg, and eye imaginal discs using digoxygenin-labeled DNA and RNA Ppt1 probes were performed. Both labeled probes reveal low ubiquitous staining indicating that Ppt1 RNA is expressed ubiquitously at a very low level (Figure S1 of Supporting Information). These results support the hypothesis that Ppt1 acts as a metabolic enzyme with housekeeping function with relatively little need for high RNA concentration and/or turnover.

To examine localization of Ppt1 protein, four chicken/rabbit polyclonal antibodies were generated against different regions of Ppt1 that include both internal sequences and the C-terminus. Embryonic, third-instar larvae, and whole adult male and female lysates were used on Western blot to test all crude sera and affinity-purified polyclonal antibodies. Results reveal that the endogenous Ppt1 protein is undetectable under standard conditions (Figure S2). To determine whether the Ppt1 polyclonal sera is specific to Ppt1, Western blot using concentrated S2 Schneider cell lysates, and adult fly head lysates (obtained via a collaboration with Dr. Robert Glaser of Wadsworth Center of NYS Department of Health) isolated from over-expressing UAS:Ppt1;P{GAL4-elav.L} flies were performed. Results indicate that only when Ppt1 is over-expressed at a high level (greater than 10 folds), or is highly enriched in S2 lysates, can a band be detected at the expected size of approximately 28 kD (Figure S2). Since Ppt1 has several conserved glycosylation sites, de-glycosylation experiment using PGNAse F (Invitrogen, Inc.) was carried out to confirm the specificity of the Ppt1 polyclonal sera. Western blot reveals a single band of ~28kD being shifted to a de-glycosylated band of 26 kD which is similar in size as the mammalian PPT1 (Figure S2; Verkruyse and Hoffmann, 1996). Since Ppt1 protein is only detected when over-expressed on a Western, it indicates that (1) the polyclonal antibodies were successful at detecting endogenous Ppt1 protein; and (2) the protein is expressed at very low levels endogeneously.

To investigate whether the loss of *Ppt1* have consequences during embryonic development, embryos homozygous for three *Ppt1* mutant strains were used: the Ppt1 null allele *Df(1)446-20*, which removes *Ppt1* and three neighboring genes [11]; and two EMS-generated alleles: $Ppt1^{A179T}$ which contains a point mutation that changed alanine 179 to threonine; and $Ppt1^{S77F}$ which contains a point mutation that changed serine 77 to phenylalanine [12]. Both EMS alleles exhibit no detectable Ppt1-specific enzyme activity. Additionally, female embryos trans-heterozygous for *Df(1)446-20* and each point mutant alleles were generated in all pair-wise combinations: $Ppt1^{A179T}$/*Df(1)446-20*, $Ppt1^{S77F}$/*Df(1)446-20*, $Ppt1^{A179T}/Ppt1^{S77F}$. We compared neural development of these embryos to those that are heterozygous for each Ppt1 strains, namely *Df(1)446-20*/+, $Ppt1^{A179T}$/+, *and* $Ppt1^{S77F}$/+.

Ppt1-deficient embryos do not display autofluorescence accumulation

INCL human patients and *Ppt1* LOF flies exhibit accumulation of autofluorescent deposits in adult brains due to the loss of protein function. Previous studies indicated that adult Ppt1 mutant fly brains exhibit larger, more abundant autofluorescent deposits than wild type and this accumulation is visible several days after pupation [12]. We also examined 14-day old wild type and Ppt1 LOF S77F adult fly brains for differences in autofluorescent deposits. As in the previous studies, our results showed that there is detectable difference in the levels of autofluorescent deposits. Although wild type adult brains display minimal deposits, Ppt1 LOF brains had more deposits visible at various wavelengths. We asked whether these accumulations are detectable during embryogenesis. Wild type and *Ppt1* LOF stage 8–17 embryos were examined for increased autofluorescent deposits in the developing nervous system. We detected no difference in the level of autofluorescence between wild type and *Ppt1*embryos at all stages examined (data not shown) indicating that the accumulation of abnormal storage materials is age-dependent and that the duration of embryogenesis is not sufficient for build-up to occur.

Ppt1 mutants display aberrant cell fate specification in early embryonic CNS development

We addressed the question of whether *Ppt1* is involved in the early events of neurogenesis- namely neural precursor specification and division. We focused on the development of some of the most well characterized neural cell lineages in the fly CNS using the mAb EVE (mAb 2B8). EVE has a defined expression patterns in ganglion mother cells (GMC) and daughter neurons of identified neural precursor lineages NB1-1, 3-3, 4-2, and 7-1 [15,16,17,18]. EVE is expressed in the first-born precursor of NB1-1, GMC1-1a, and its progeny, the aCC and pCC motoneurons; the EL neurons deriving from NB3-3; GMC4-2 and its daughter neurons RP2 motoneuron and its sib from NB4-2, and the U/CQ neurons deriving from NB7-1.

Results indicate that *Ppt1* mutant embryos display abnormal complement of EVE+ GMCs and their progeny in many hemisegments, as early as stage 11/12 of embryogenesis. At stage 11–12, EVE is expressed in GMCs that produce the RP2 motoneuron and its sib; aCC/pCC and U/CQ neurons (Figure 1A). *Ppt1* mutant embryos from *Df(1)446-20*, $Ppt1^{A179T}$, *and* $Ppt1^{S77F}$, and trans-heterozygous *Ppt1* mutant crosses show a variety of phenotypes. Some embryos display cellular disorganization where EVE+ GMCs are displaced. In others, there is a loss or gain of extra EVE-positive GMCs and neurons in many hemisegments (Figure 1B–E). The most prevalent phenotype is the loss of GMC4-2.a, the parental precursor that will give rise to the RP2 motoneuron. Occasionally, extra U/CQ and aCC/pCC GMCs are also observed as also the presence of extra RP2s or its sib after GMC4-2.a has divided (Figure 1D–E). Overall, 31% (n = 42) of *Ppt1*- embryos display abnormality at stage 12. Later in embryonic development during stage 14–15 when the EVE+ GMCs give rise to EVE+ neurons, the loss of EVE+ RP2s is observed in a small, but significant percentage of hemisegments in *Ppt1*mutants (Figure 2; Table 1). Specifically, over 36% of T1-A8 hemisegments show a loss of RP2s in *Df(1)446-20* embryos. Point

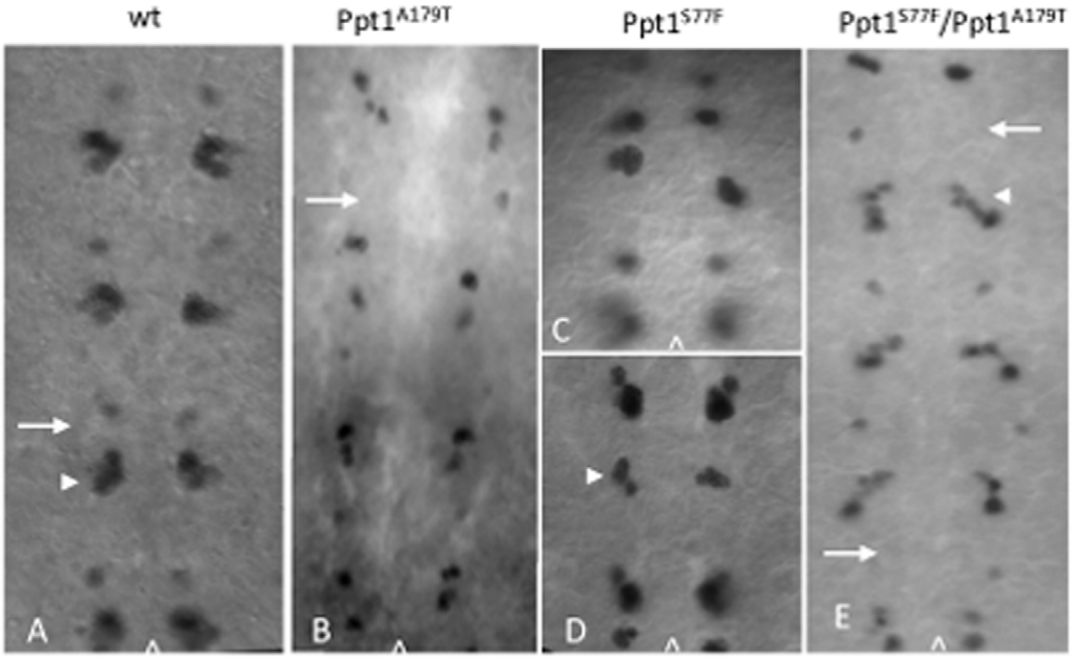

Figure 1. *Ppt1* LOF mutants exhibit abnormal complement of EVE+ neural precursors and neurons. (A) In wild type, EVE is expressed in GMC4-2.a, the neural precursor that give rise to RP2 motoneuron and its sib (arrow); and in a cluster of GMCs that give rise to the aCC, pCC, CQ neurons (arrowhead). (B–E) In *Ppt1* mutants, many hemisegments exhibit a variety of phenotype including the loss of GMC4.2a (arrow in B and E), extra RP2/sib neurons (arrowhead in D), disorganized EVE+ clusters (C), and extra aCC/pCC cells (arrowhead in E). In all panels, embryos are at S11–12 of development; anterior, up; caret, midline.
doi:10.1371/journal.pone.0014402.g001

mutants and trans-heterozygous embryos show 12–17% loss in all hemisegments (Table 1). The degree of penetrance of this EVE neural phenotype is variable: all *Df(1)446-20* embryos show at least two missing RP2s whereas $Ppt1^{A179T}$ *and* $Ppt1^{S77F}$ point mutations range from 32–50%. 63% of embryos from $Ppt1^{A179T}$×*Df(1)446-20* trans-heterozygous crosses and 27% of $Ppt1^{S77F}$×*Df(1)446-20* trans-heterozygous crosses display a partial loss of EVE+ RP2 neurons (Figure 2; Table 2). In contrast, all Ppt1 mutant strains outcrossed to wild type Oregon-R, *Df(1)446-20*/+, $Ppt1^{A179T}$/+, *and* $Ppt1^{S77F}$/+, all showed normal EVE expression (Tables 1 and 2). These results indicate that the EVE phenotypes are due to the loss of Ppt1.

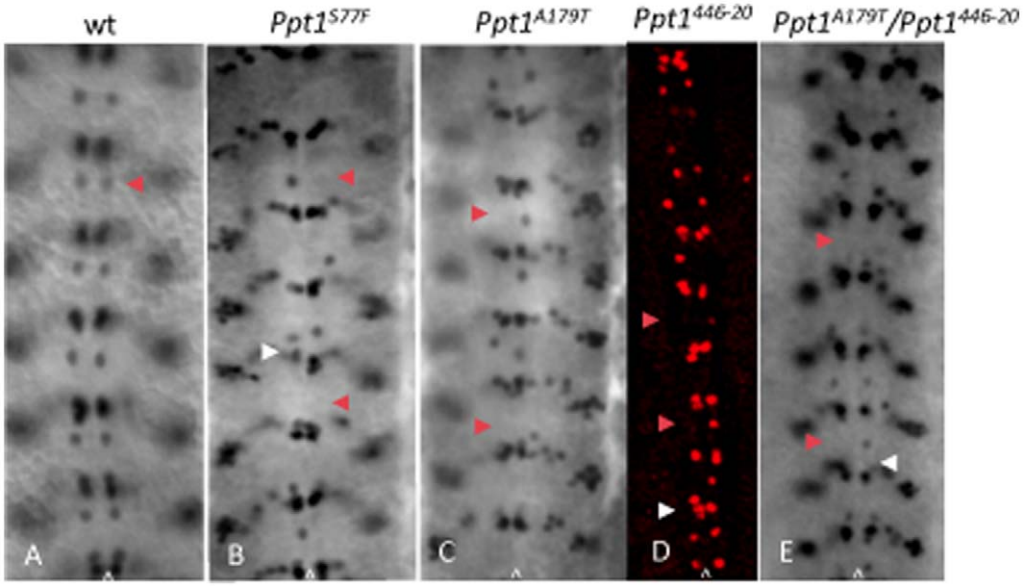

Figure 2. Loss of *Ppt1* results in missing EVE+ RP2 neurons in many hemisegments of S16 embryonic CNS. Arrowhead indicates RP2 neuron in all panels. (A). Wild type EVE+ CNS pattern. (B–E) *Ppt1* LOF mutants exhibit a variety of phenotype including the loss of EVE+ RP2s in some hemisegments (red arrowhead in B–E), disorganized or missing aCC/pCC clusters (white arrowhead in B, D and E). Anterior, up; caret, midline.
doi:10.1371/journal.pone.0014402.g002

Table 1. Percentage of hemisegments in *Ppt1*-deficient embryos with missing EVE+ RP2 neurons.

genotype	%	n
wild type	0	220
$Ppt1^{Df(1)446\text{-}20}$	36.4	220
$Ppt1^{Df(1)446\text{-}20}$/+	0	220
$Ppt1^{A179T}$	16	198
$Ppt1^{A179T}$/+	0	220
$Ppt1^{S77F}$	17	198
$Ppt1^{S77F}$/+	0	220
$Ppt1^{S77F}/Ppt1^{Df(1)446\text{-}20}$	12	220
$Ppt1^{A179T}/Ppt1^{Df(1)446\text{-}20}$	12	374

n, number of hemisegments at stage 14–16.
doi:10.1371/journal.pone.0014402.t001

EVE is also essential for normal axonal guidance and innervation of the RP2 motoneuron [19] thus EVE can provide clues as to whether the observed alterations in cell fate lead to faulty axon pathfinding and innervation. To verify the mis-specification of neuronal cell fates in the EVE+ lineages as well as to assess the RP2 axonal projections, *Df(1)446-20* and $Ppt1^{A179T}$ flies were crossed to lines bearing either the *UAS-tau-LacZ* or *UAS-CD8-GFP* reporter (*RN2-Gal4:UAS-CD8-GFP or RN2-GAL4:UAS-tau-LacZ*) driven by the RP2/aCC/pCC-specific Gal4 driver (*RN2-Gal4*) to clearly mark the cell bodies and axons of aCC and pCC, and RP2 neurons [20]. Anti- β-gal staining and GFP visualization of embryos from these crosses confirmed EVE staining results. *Ppt1;RN2-Gal4:UAS-CD8-GFP* and *Ppt1; RN2-Gal4:UAS-tauLacZ* embryos display a loss of either *tau*LacZ or GFP-expressing RP2s and aCC/pCC neurons in many hemisegments; and disorganized cellular arrangements of the remaining LacZ-positive neurons. In many *Ppt1* mutants, the remaining RP2 motoneuron exhibits abnormal axon trajectory (Figure 3). Normally at late embryogenesis, the RP2 motoneuron extends its axon anteriorly toward the ipsilateral neighboring anterior segment to join the intersegmental nerve (ISN) to exit the CNS and eventually synapsing onto the dorsal muscle (Figure 3A). In many $Ppt1^{A179T}$; *UAS-tauLacZ* embryos, the RP2 neurons extend its axons in the wrong direction-posteriorly to join the posterior ipsilateral ISN instead (Figure 3D) while other RP2 axons project contralaterally toward the midline, stalled, and never exit the CNS (Figure 3E). These embryos also display a loss of either aCC or pCC neurons in many hemisegments (Figure 3B–E). Collectively, these studies indicated that the loss of *Ppt1* caused abnormal neuronal cell fate specification and defective axon pathfinding.

Table 2. Penetrance of EVE+ RP2 phenotype in *Ppt1*-embryos.

genotype	%	n
wild type	0	30
$Ppt1^{Df(1)446\text{-}20}$	100	25
$Ppt1^{Df(1)446\text{-}20}$/+	0	10
$Ppt1^{A179T}$	50	18
$Ppt1^{A179T}$/+	0	10
$Ppt1^{S77F}$	32	28
$Ppt1^{S77F}$/+	0	10
$Ppt1^{S77F}/Ppt1^{Df(1)446\text{-}20}$	27	37
$Ppt1^{A179T}/Ppt1^{Df(1)446\text{-}20}$	63	24

%, percentage of stage 15–16 embryos with 2 or more missing RP2s.
n, number of embryos scored.
doi:10.1371/journal.pone.0014402.t002

Embryonic glial development is normal in *Ppt1* mutants

Since neuronal and glial development are temporally and spatially linked and can be derived from a common neuronal precursor (e.g. NB1-1 produces both aCC/pCC neurons as well as the A and B glia located dorsally on the CNS [21]), glial development was examined using the glial-specific marker REPO (mAb 8D12). The evolutionary conserved REPO protein is expressed in most glia in the embryonic CNS and PNS. During embryogenesis, REPO is essential for the migration and differentiation of glia, particularly the longitudinal glia of the CNS and the exit glia of the PNS. All *Ppt1* LOF mutants exhibit normal REPO-positive glia; thus *Ppt1* is not essential for the specification of embryonic glia (data not shown).

Ppt1 mutants exhibit variable embryonic CNS and PNS axonal defects

Overall axon guidance and fasciculation during neural development were examined using a number of axonal markers, BP102, FUTSCH (mAb22C10), and Fasciclin II (mAb1D4). In wild type, the axon tracts of the embryonic CNS consist of two longitudinal axon bundles running lengthwise along the ventral nerve cord intersected by segmentally reiterated pairs of anterior and posterior commissures that crosses the midline at every segment (Figure 4A). The CNS axon scaffold can be visualized using BP102 which recognizes a carbohydrate epitope present on all CNS axons [22]. 73% of *Df(1)446-20*, 35% of $Ppt1^{A179T}$, and 24% of $Ppt1^{S77F}$ embryos show mild to severe defects (Figure 4; Table 3). Mild defects include irregularly spacing of the ventral nerve cord, some disorganization of the axon scaffold, abnormally thin or thick, and wavy longitudinal connectives. Moderate defects include narrowing of spaces between the commissures (Figure 4B), broader and/or more compressed anterior and posterior commissures, and interrupted, frayed longitudinal connectives (Figure 4C). Severe defects observed include severe disorganization of the longitudinal tracts at many segments, the complete loss of longitudinal connectives in other segments, and fused or missing commissures (Figure 4C & D).

To evaluate the morphology of a more discrete subset of axonal longitudinal connectives, *Df(1)446-20*, $Ppt1^{A179T}$, *and* $Ppt1^{S77F}$, and trans-heterozygous *Ppt1* mutant embryos were stained with mAb1D4. At stage 17, mAb1D4 recognizes the neural adhesion protein Fasciclin II, which is expressed in three discrete axon longitudinal bundles on either side of the midline (Figure 5A; [23]). 50–58% of *Ppt1* mutant embryos display abnormal FasII-positive longitudinal connectives ranging from mild to severe (Table 3). Mild defects include loose and defasciculated connectives, wavy in appearance. More severe FasII defects include ectopic midline crossing of the longitudinal connectives, discontinuous connectives in all three FasII bundles, and frayed connectives due to defasciculation (Figure 5B).

We examine the specific requirement of *Ppt1* in neurons by driving the expression of *Ppt1*-RNAi in strains containing the ds RNA-GD3286 construct (obtained from the Vienna *Drosophila* RNAi Center [24]); and the dsRNA-JF01972 construct from the TriP-1 collection (Bloomington Drosophila Stock Center) using various neural-specific Gal4 drivers (Bloomington Drosophila

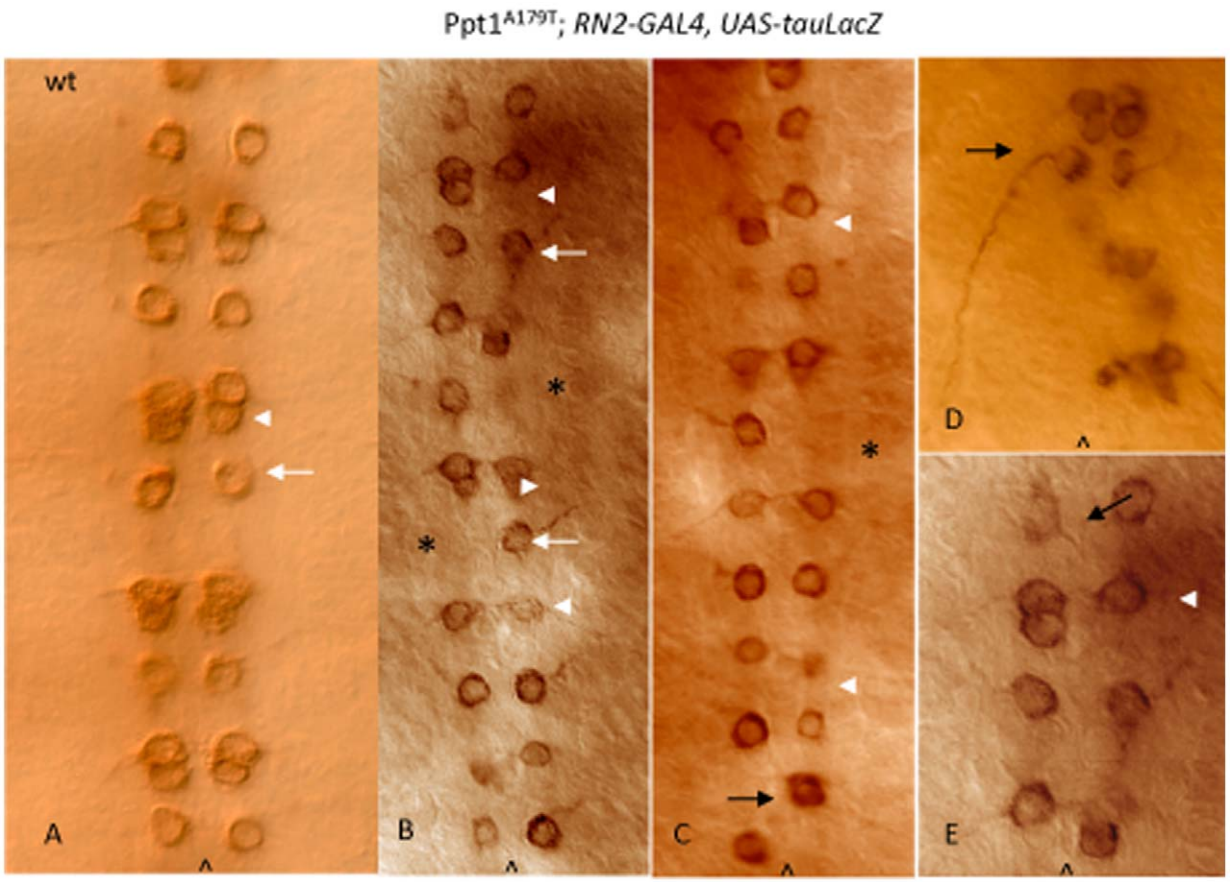

Figure 3. *Ppt1* mutants exhibit abnormal RP2 axon trajectories. S16 ventral nerve cord stained with anti-β-gal to detect RN2-*tau-lacZ* expressed in aCC, pCC and RP2 neurons. (A) Wild type RN2-*tau-lacZ* pattern showing RP2 neuron and its axon trajectory (white arrow); and aCC/pCC neurons (arrowhead). (B–D). *Ppt1*^{A179T}; RN2-Gal4:UAS-*tauLacZ* embryos display a loss of RP2 motoneurons (asterisks) and aCC/pCC neurons (arrowheads) in many hemisegments; and disorganized cellular arrangements of the remaining LacZ-positive neurons. Many hemisegments have normal RP2 axon trajectory (white arrow) while others do not (black arrow). The RP2 in panel C shows an abnormal axon trajectory projecting posteriorly instead of anteriorly. Panel E is an enlarged subset of B. Anterior, up; caret, midline.
doi:10.1371/journal.pone.0014402.g003

Stock Center). The dsRNA-GD3286 construct recognizes 310 nucleotides within the first exon of the Ppt1 gene; the dsRNA-JF01972 construct recognizes 531 nucleotides-nearly all the first exon of the gene. Ppt1-RNAi embryos were examined for *Ppt1*-associated FasII defects. 85–100% *Ppt1*RNAi-*elav*-Gal4 embryos display defects ranging from mild to severe axon bundles (Figure 5C and D; Table 4). Similarly, 85% of *Ppt1*RNAi- U/CQ-Gal4 and 93% *Ppt1*RNAi-aCC/RP2-Gal4 embryos exhibit varying degrees of axon defects ranging from wavy but intact bundles; to frayed, discontinuous or missing bundles in many hemisegments. In contrast, embryos from the parental strains exhibit normal axon patterns (Table 5). These results collectively indicate that *Ppt1* is essential in the neurons for proper axon guidance and fasciculation.

The developing PNS of *Ppt1* mutants also show neuronal defects as assayed by 22C10, an antibody that recognizes the cytoskeletal FUTSCH protein found in the cytoplasm of a subset of CNS and PNS neurons and axons as well as their projections [25]. Normally, FUTSCH is expressed in the cell bodies as well as the axons and dendrites of 44 PNS neurons per abdominal segment [26]. 22C10-positive PNS neurons include the dorsal cluster (d), the ventral and ventral' cluster (v and v′), and the lateral cluster which consists of five chordotonal organs (lch5). Wild type and *Ppt1* LOF embryos showed no detectable difference in the number of neurons or axon projections in the l, v, and v′ neuron clusters. However, the lch5 neurons showed a variety of defects including decreased number of sensory neurons, fused and abnormally shaped neurons, and disorganized clusters with aberrant dendritic projections (Figure 6; Table 5). Occasionally, fasciculation defects with abnormal axonal connections between **v′** clusters and ISN are observed (data not shown). These findings indicate that lch5 neuron clusters are preferentially more sensitive than l, v, and v′ clusters to the loss of *Ppt1*.

Discussion

RNA and antibody expression results reveal the low abundance nature of Ppt1 RNA and protein confirming what was previous thought- Ppt1 is an essential housekeeping gene. Because of its low abundance, we are unable to ascertain the subcellular localization of Ppt1 and thus could not determine whether fly Ppt1 is lysosomal, synaptic, or both. To address this question, Ppt1 would need to be over-expressed by at least 17-folds to be at a marginally detectable level using immunofluorescence. This is not ideal since Ppt1 over-expression leads to apoptosis. Our studies clearly indicate that Ppt1 protein is expressed ubiquitously at a very low level such that only a minute amount is required for function. Whether this minute amount of protein resides predominantly in

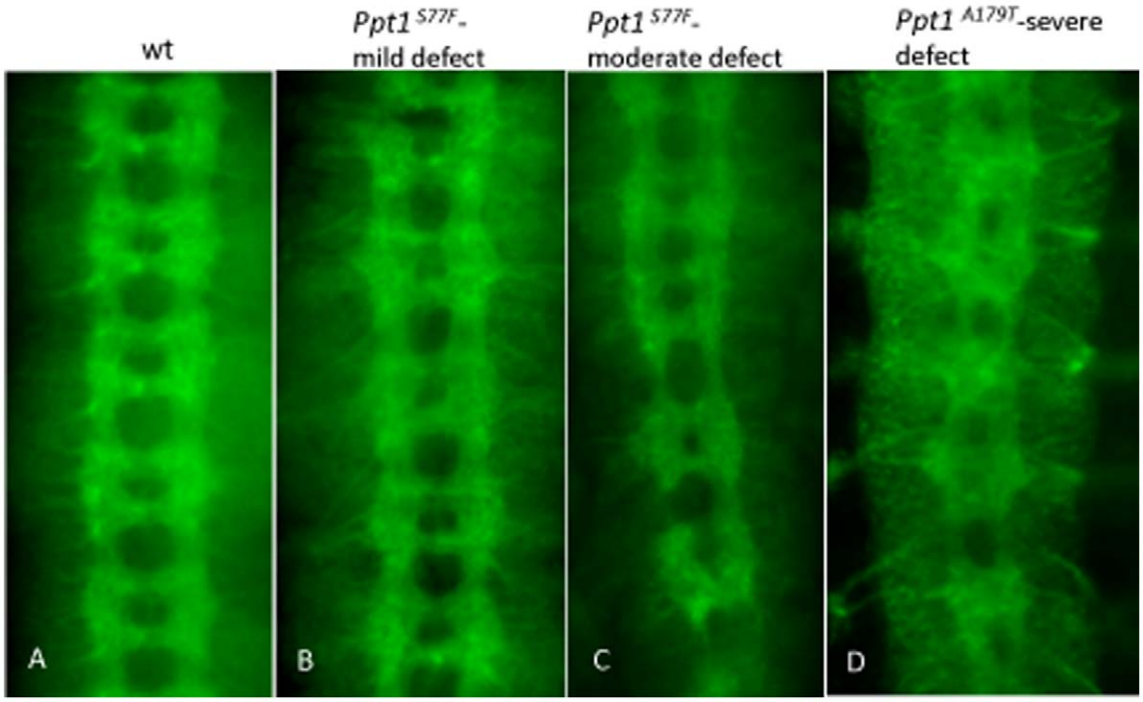

Figure 4. CNS scaffold abnormalities in *Ppt1* mutant embryos. In all panels, S16 embryos were stained with BP102. (A) Wild type embryo. (B) Axon defects range from mild phenotypes such as irregularly spaced axon tracts in commissures and wavy, thinning longitudinal connectives; to more severe phenotype such as fused commissures and disorganized CNS tracts (C and D). Anterior, up.
doi:10.1371/journal.pone.0014402.g004

the lysosomes and/or synapses for the turnover of palmitoylated developmental proteins, it is necessary and its absence would most likely have similar consequences.

Our results indicate that *Ppt1* is essential at a time when neural precursors are being determined, one of the earliest stages of embryonic neural development. Small discreet defects were detected early shortly after gastrulation with the alteration in CNS neural precursor cell fates in a number of identified neural precursors. Specifically, the phenotype is limited to a discreet subset of EVE+ neural lineages (e.g. the neuroblast lineage giving rise to RP2s, aCC and pCC neurons); while other EVE+ cells such as U's and EL interneurons are normal. In the affected lineages, the loss of *Ppt1* has small consequences at the early cell determination stage such that only a subset of all EVE+ RP2s, aCC/pCC neurons are affected. This indicates that even at this very early stage of neurogenesis, Ppt1-mediated protein turnover is essential. Neural defects increase as development proceeds such that by mid-to–late embryogenesis, malformed neurons and abnormal longitudinal axon tracts are visible in nearly all *Ppt1*-deficient embryos. Specifically, the development of the RP2, aCC and pCC neurons requires *Ppt1*; most likely through regulating EVE expression. Without *Ppt1*, many RP2, aCC/pCC neurons are abnormally positioned or missing; while some exhibit aberrant axon projections. Since EVE regulates proper axon projections in the developing CNS, particularly dorsally projecting aCC and RP2 motoneurons (pCC is an interneuron), this phenotype is wholly unexpected. These pathfinding and fasciculation defects reflect what we suspect: Ppt1-mediated turnover of palmitoylated developmental proteins is necessary throughout development such that its loss is cumulative and progressive. This is supported by previous studies showing that young adult brains exhibit age-dependent abnormal autofluorescence deposits due to the absence of *Ppt1* [12]. Neurons, in particular, exhibit a high rate of palmitoylation-depalmitoylation dynamics due to its high level of signal transduction and protein trafficking through neurotransmitter release. Since there are numerous endosomal/lysosomal pathways, the loss of one protein would not necessarily result in massive disturbances but may limit the number of protein turnovers and recycling which may cause a "domino" effect by directly or indirectly disrupting downstream pathways during neural development.

Table 3. Percentage of *Ppt1*-deficient embryos displaying axonal defects.

Antibody staining	*Wild type*	*Df(1)446-20*	$Ppt1^{A179T}$	$Ppt1^{S77F}$
anti-BP102	0% (6)	73% (34)	35% (34)	12% (49)
anti-fasII (1D4)	0% (11)	58% (36)	50% (46)	n/d
Anti-FUTSCH (22C10)	0% (10)	70% (50)	60.5% (38)	n/d

Parentheses, the number of stage 16–17 embryos assayed.
n/d: not determined.
doi:10.1371/journal.pone.0014402.t003

Downstream targets of *Ppt1* during neurogenesis are largely unknown. A previous study indicates that FasII, a neural adhesion protein, may be a candidate [14]. *Ppt1* over-expression screens have isolated FasII as a potential *Ppt1*-interacting protein. Our results showed that *Ppt1*-deficient embryos display FasII-specific axon fasciculation defects. FasII, a homolog of the vertebrate NCAM, is a palmitoylated protein and serves as a second anchor for proteins involved in N-CAM mediated signaling at the membrane [27]. Fasll has also been shown to interact with lipid rafts to mediate FGF signaling to promote neurite outgrowth [28]. Perhaps Fasll plays a similar role during

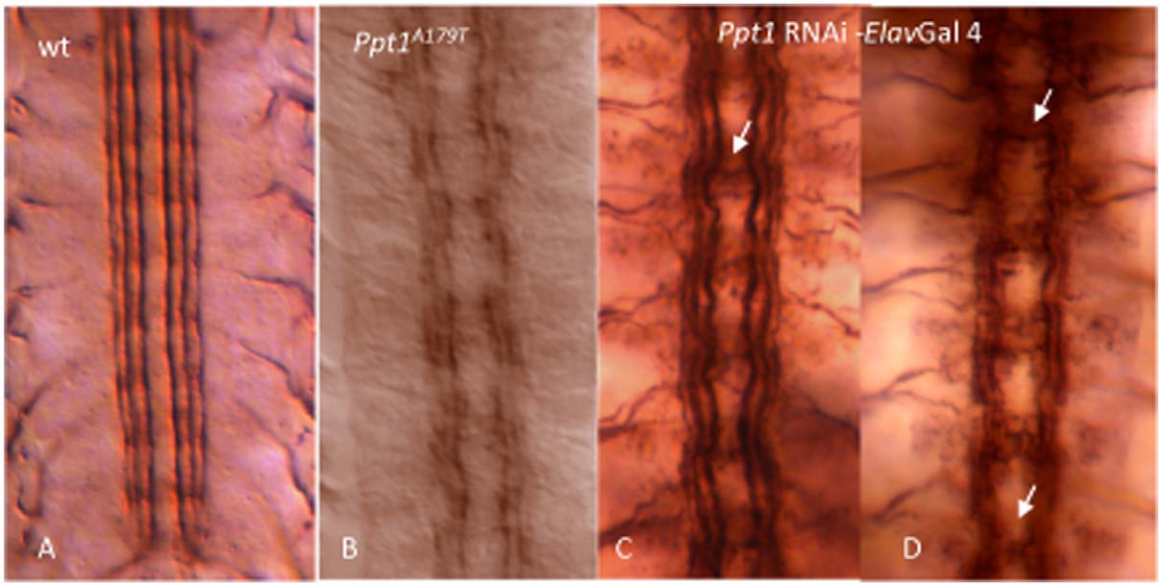

Figure 5. Mutant *Ppt1* and *Ppt1* RNAi knock-down in neurons result in defective axon tracts in the developing CNS. In all panels, S17 embryos were stained with 1D4 antibody. (A) FASII is expressed in three longitudinal connectives at this stage. (B) $Ppt1^{A179T}$ embryos exhibit discontinuous and frayed longitudinal connectives. (C, D) *Ppt1* RNAi expression under the control of *elav* gal4 driver results in a range of axon guidance phenotype including wavy bundles with some faulty axon crossing over the midline (arrow in C); and disorganized and/or broken connectives, and fused commissures (arrows in D). Anterior, up.
doi:10.1371/journal.pone.0014402.g005

fly neurogenesis where it is involved in lipid raft-mediated signaling. Since *Ppt1* has been suggested to also facilitate cell signaling via its localization to lipid rafts [29], FasII may require *Ppt1*-mediated palmitoylation turnover at the membrane to regulate the integration of signaling required to insure proper axon outgrowth and fasciculation.

The loss of *Ppt1* has varied consequences from the loss or gain of neurons, axon fasciculation defects, to axon guidance in a subset of motor neurons (e.g. RP2, aCC), sensory neurons, and interneurons (e.g. pCC but not the EL interneurons). This observation is analogous to what is observed in INCL humans and animal models. INCL patients undergo progressive degeneration in selective areas of the brain while leaving others intact. PPT1-deficient adult mice exhibit the loss of GABAergic interneurons in discrete regions of the brain [10] and thalamic neurons [30] months prior to being symptomatic. It is presently unclear whether PPT1-deficiencies affect mice earlier, during embryonic neural development.

Table 4. Quantitation of *Ppt1* RNAi embryos displaying FasII defects.

genotype	% defective
$Ppt1^{5499}$RNAi	0.03 (30)
$Ppt1^{25952}$TRiP RNAi	0 (30)
elav-gal4	0 (33)
UAS *tauLacZ CQ2*-gal4	0 (30)
UAS *tauLacZ RN2*-gal4	0 (35)
$Ppt1^{5499}$RNAi×*elav*-gal4	100 (81)
$Ppt1^{25952}$TRiP RNAi×*elav*-gal4	85.7 (42)
$Ppt1^{5499}$RNAi×UAS *tauLacZ CQ2*-gal4	85 (67)
$Ppt1^{5499}$RNAi×UAS *tauLacZ RN2*-gal4	93.4 (106)

Parentheses, the number of stage 16–17 embryos assayed.
Ppt1 RNAi expression is driven by the following neural specific Gal4 drivers: *elav-gal4*-drives expression in CNS and PNS neurons.
UAS tau-LacZ CQ2-gal 4 driver- drives tau-LacZ expression in U/CQ neurons.
UAS tau-LacZ RN2-gal 4 driver- drives *tau-LacZ* expression in aCC and RP2 neurons.
doi:10.1371/journal.pone.0014402.t004

The low penetrance of *Ppt1* phenotype indicates that the loss of *Ppt1* is generally well tolerated perhaps due to the presence of compensatory mechanisms. A closely related sister gene, PPT2, exists in mammals [31] and in *Drosophila*. PPT2 knock-out mice display many of the same INCL phenotype and pathology including spasticity and autofluorescence accumulation in the brain [32]. We are currently investigating whether the PPT2 fly homolog, *Ppt2*, also have an embryonic neural phenotype and whether *Ppt1/Ppt2* double mutants have a more severe phenotype than the single mutation.

Materials and Methods

Drosophila Strains

Ppt1 LOF mutant alleles $Ppt1^{A179T}$, $Ppt1^{S77F}$, and the *Df(1)446-20* deficiency line were provided by Dr. Robert Glaser (Wadsworth Center, NYS Department of Health, Albany, NY). Oregon-R, w^*; P{RN2-GAL4}P, P{UAS-tau-lacZ.B}2 and w^*; P{RN2-GAL4}P, P{UAS-mCD8::GFP.L}LL5 , *Elav*-Gal4 driver, U/CQ-Gal4 driver, aCC/RP2-Gal4 driver, and *Ppt1*-RNAi TRiP line, and Oregon-R were obtained from Bloomington Drosophila Stock Center. *Ppt1*- UAS RNAi flies (w1118; P{GD3286} [14]) was obtained from Vienna *Drosophila* RNAi Center (Vienna, Austria). All strains were maintained on standard *Drosophila* cornmeal-yeast medium at 25°C.

To detect autofluorescence deposits, brains from 14-day old Oregon-R and $Ppt1^{S77F}$ were extracted and immediately examined on a Leica SP2 confocal microscope for comparison.

Table 5. Quantitation of *Ppt1* axon defects in the embryonic CNS and PNS.

phenotype	*Wild type*	*Ppt1*^{A179T}	*Ppt1*$^{446-20}$	*Ppt1*^{5499}RNAi× *elav*-gal4	*Ppt1*^{25952}TRiP RNAi×*elav*-gal4	*Ppt1*^{5499}RNAi×UAS *tauLacZ CQ2*-gal4	*Ppt1*^{5499}RNAi×UAS *tauLacZ RN2*-gal4
PNS							
Irregular spacing of lch5 neuron clusters	0	6	6	n/d	n/d	n/d	n/d
Missing lch5 neurons	0	4	6	n/d	n/d	n/d	n/d
Malformed lch5 neurons	0	13	13	n/d	n/d	n/d	n/d
CNS							
slightly irregular and/ or wavy longitudinal tracts	0	31	21	40	9	25	7
Discontinuous, frayed longitudinal tracts	0	8	11	35	33	35	99
Irregular, missing or fused commissures	0	16	17	6	14	7	10
Total number of embryos scored	27	69	58	81	42	67	106

-number of embryos of each genotype displaying various fasII and 22C10 defects; many embryos exhibit combination of phenotypes.
n/d: not determined.
doi:10.1371/journal.pone.0014402.t005

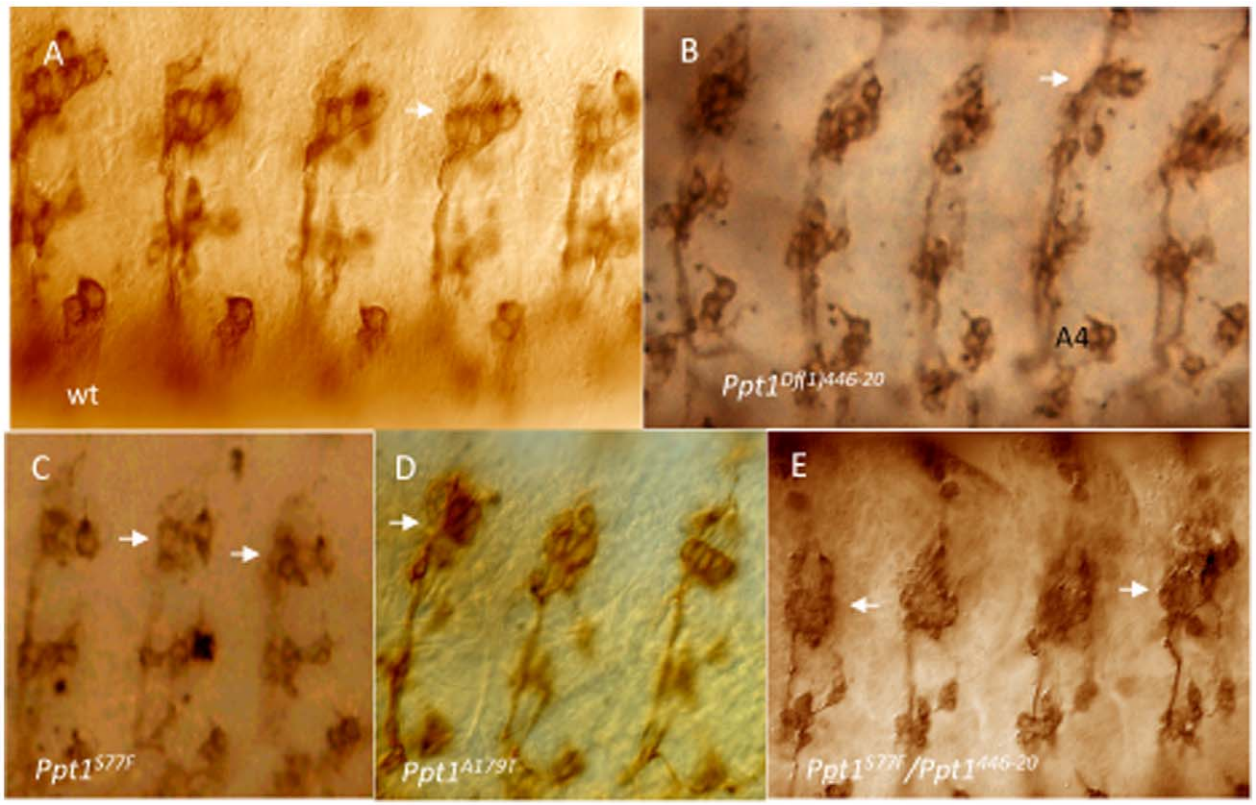

Figure 6. Chordotonal neurons (lch5) in the developing PNS are abnormal in many *Ppt1* LOF embryos. In all panels, lch5 neurons are indicated by the arrows. Side view of S17 embryos stained with Mab 22C10. (A) Wild type clusters of lch5, v, and v′ neurons are located in every abdominal segment. (B–E) lch5 neurons in mutant *Ppt1* embryos demonstrate a variety of defects: decreased number of neurons (B), fused and abnormally shaped (D, E), organization and positional defects, and thin axon bundles (black arrowhead) (B and C). dorsal, up.
doi:10.1371/journal.pone.0014402.g006

Immunocytochemistry and Immunofluorescence

Embryos were fixed and stained according to previously described methods [33,34], and using the following primary antibodies obtained from University of Iowa Developmental Studies Hybridoma Bank: mAb 22C10 (1:50), mAb BP102 (1:50), mAb 2B8 (1:30), and mAb 1D4 (1:5). β-gal monoclonal antibody at 1:1000 obtained from Jackson ImmunoResearch, Inc. Immunocytochemical detection was performed using HRP-conjugated goat anti-mouse secondary antibody (1:300; Jackson ImmunoResearch, Inc.). Immunofluorescence was performed using Alexa-488 and Alexa-594 conjugated goat anti-mouse secondary antibodies (1:300; Molecular Probes/ Invitrogen, Inc.). For each genotypic staining of EVE, 100–200 thoracic and abdominal hemisegments from at least 20 appropriately staged embryos were counted. Digital images of stained embryos were captured using either the Advanced Color SPOT system or the Retiga EXi Fast 1394 mounted onto a Nikon E600 compound microscope.

Supporting Information

Figure S1 Whole mount *in situ* RNA hybridization reveals that *Ppt1* transcript is ubiquituously expressed at low levels during (A) embryogenesis and (B) 3rd instar imaginal discs. 0–16 hours wild type embryos and 3rd instar imaginal discs were collected, fixed and hybridized with digoxygenin-labeled anti-sense *Ppt1* RNA probes. Anti-sense RNA probes were generated from a CG12108 cDNA clone GM21019 (Research Genetics). Embryo *in situ* hybridization was performed using standard protocols.
Found at: doi:10.1371/journal.pone.0014402.s001 (0.82 MB PDF)

Figure S2 Western blot using affinity-purified Ppt1 polyclonal antibody (generated against the C-terminus) of S2 cell lysate, wild type W1118 fly head extract (arrows), and over-expressed Gal4-UAS-Ppt1 head extract untreated (A) and treated with pGNAse (B) to remove N-glycosylation. Results indicate that although no band is detected in the S2 lysate and W1118 lanes (arrows), Ppt1 antibody is specific to Ppt1 protein and can be detected when Ppt1 is over-expressed (A and B). Two rabbit and two chicken polyclonal antibodies were generated using the following peptides located in the internal region of the *Ppt1* gene: VAERCP-NPPMRNLIT, ATYWHDPIMENKYR, and IVQPKESQWF-QYYTT ; and VYQNLGLDKMHRQGQ located at the C-terminal region (GeneMed Synthesis, Inc.; Aves Laboratories, Inc.). Affinity purifications were performed using the Pierce Biotechnology SulfoLink (#20405) and AminoLink kit (#44890) according manufacturer's standard protocols. Western blot was performed using the ECL Western Blotting Analysis System (Pierce Biotechnology). Deglycosylation experiments were performed using lysates prepared from S2 Schneider cells, and adult fly heads from W1118 and UAS:Ppt1 2.1/GMR:GAL4 flies. Samples were treated with PGNase F according to manufacturer's instruction (glycerol free kit #P0705S; New England Biolabs, Inc.) prior to Western Blotting.
Found at: doi:10.1371/journal.pone.0014402.s002 (0.29 MB PDF)

Acknowledgments

We acknowledge Bob Glaser for *Ppt1* LOF mutant fly strains; Kris Korey for UAS:Ppt1;P{Gal4Elav} flies; Jim Skeath, John LaGraff, and three anonymous reviewers for comments on the manuscript.

Author Contributions

Conceived and designed the experiments: QCL. Performed the experiments: CB PO CD. Analyzed the data: QCL CB. Wrote the paper: QCL.

References

1. Cooper JD (2003) Progress towards understanding the neurobiology of Batten disease or neuronal ceroid lipofuscinosis. Curr Opin Neurol 16: 121–128.
2. Mole S, Gardiner M (1999) Molecular genetics of the neuronal ceroid lipofuscinoses. Epilepsia 40 Suppl 3: 29–32.
3. Camp LA, Hofmann SL (1993) Purification and properties of a palmitoyl-protein thioesterase that cleaves palmitate from H-Ras. J Biol Chem 268: 22566–22574.
4. Camp LA, Verkruyse LA, Afendis SJ, Slaughter CA, Hofmann SL (1994) Molecular cloning and expression of palmitoyl-protein thioesterase. J Biol Chem 269: 23212–23219.
5. Isosomppi J, Heinonen O, Hiltunen JO, Greene ND, Vesa J, et al. (1999) Developmental expression of palmitoyl protein thioesterase in normal mice. Brain Res Dev Brain Res 118: 1–11.
6. Suopanki J, Tyynela J, Baumann M, Haltia M (1999) The expression of palmitoyl-protein thioesterase is developmentally regulated in neural tissues but not in nonneural tissues. Mol Genet Metab 66: 290–293.
7. Heinonen O, Kyttala A, Lehmus E, Paunio T, Peltonen L, et al. (2000) Expression of palmitoyl protein thioesterase in neurons. Mol Genet Metab 69: 123–129.
8. Lehtovirta M, Kyttala A, Eskelinen EL, Hess M, Heinonen O, et al. (2001) Palmitoyl protein thioesterase (PPT) localizes into synaptosomes and synaptic vesicles in neurons: implications for infantile neuronal ceroid lipofuscinosis (INCL). Hum Mol Genet 10: 69–75.
9. Ahtiainen L, Van Diggelen OP, Jalanko A, Kopra O (2003) Palmitoyl protein thioesterase 1 is targeted to the axons in neurons. J Comp Neurol 455: 368–377.
10. Jalanko A, Vesa J, Manninen T, von Schantz C, Minye H, et al. (2005) Mice 0with Ppt1Deltaex4 mutation replicate the INCL phenotype and show an inflammation-associated loss of interneurons. Neurobiol Dis 18: 226–241.
11. Glaser RL, Hickey AJ, Chotkowski HL, Chu-LaGraff Q (2003) Characterization of Drosophila palmitoyl-protein thioesterase 1. Gene 312: 271–279.
12. Hickey AJ, Chotkowski HL, Singh N, Ault JG, Korey CA, et al. (2006) Palmitoyl-protein thioesterase 1 deficiency in Drosophila melanogaster causes accumulation of abnormal storage material and reduced life span. Genetics 172: 2379–2390.
13. Korey CA, MacDonald ME (2003) An over-expression system for characterizing Ppt1 function in Drosophila. BMC Neurosci 4: 30.
14. Buff H, Smith AC, Korey CA (2007) Genetic modifiers of Drosophila palmitoyl-protein thioesterase 1-induced degeneration. Genetics 176: 209–220.
15. Chu-LaGraff Q, Doe CQ (1993) Neuroblast specification and formation regulated by wingless in the Drosophila CNS. Science 261: 1594–1597.
16. Broadus J, Doe CQ (1995) Evolution of neuroblast identity: seven-up and prospero expression reveal homologous and divergent neuroblast fates in Drosophila and Schistocerca. Development 121: 3989–3996.
17. Bossing T, Udolph G, Doe CQ, Technau GM (1996) The embryonic central nervous system lineages of Drosophila melanogaster. I. Neuroblast lineages derived from the ventral half of the neuroectoderm. Dev Biol 179: 41–64.
18. Schmidt H, Rickert C, Bossing T, Vef O, Urban J, et al. (1997) The embryonic central nervous system lineages of Drosophila melanogaster. II. Neuroblast lineages derived from the dorsal part of the neuroectoderm. Dev Biol 189: 186–204.
19. Landgraf M, Roy S, Prokop A, VijayRaghavan K, Bate M (1999) even-skipped determines the dorsal growth of motor axons in Drosophila. Neuron 22: 43–52.
20. Fujioka M, Lear BC, Landgraf M, Yusibova GL, Zhou J, et al. (2003) Even-skipped, acting as a repressor, regulates axonal projections in Drosophila. Development 130: 5385–5400.
21. Udolph G, Prokop A, Bossing T, Technau GM (1993) A common precursor for glia and neurons in the embryonic CNS of Drosophila gives rise to segment-specific lineage variants. Development 118: 765–775.
22. Seeger M, Tear G, Ferres-Marco D, Goodman CS (1993) Mutations affecting growth cone guidance in Drosophila: genes necessary for guidance toward or away from the midline. Neuron 10: 409–426.
23. Grenningloh G, Bieber AJ, Rehm EJ, Snow PM, Traquina ZR, et al. (1990) Molecular genetics of neuronal recognition in Drosophila: evolution and function of immunoglobulin superfamily cell adhesion molecules. Cold Spring Harb Symp Quant Biol 55: 327–340.
24. Dietzl G, Chen D, Schnorrer F, Su KC, Barinova Y, et al. (2007) A genome-wide transgenic RNAi library for conditional gene inactivation in Drosophila. Nature 448: 151–156.
25. Zipursky SL, Venkatesh TR, Benzer S (1985) From monoclonal antibody to gene for a neuron-specific glycoprotein in Drosophila. Proc Natl Acad Sci U S A 82: 1855–1859.

26. Bodmer R, Carretto R, Jan YN (1989) Neurogenesis of the peripheral nervous system in Drosophila embryos: DNA replication patterns and cell lineages. Neuron 3: 21–32.
27. Little EB, Edelman GM, Cunningham BA (1998) Palmitoylation of the cytoplasmic domain of the neural cell adhesion molecule N-CAM serves as an anchor to cellular membranes. Cell Adhes Commun 6: 415–430.
28. Niethammer P, Delling M, Sytnyk V, Dityatev A, Fukami K, et al. (2002) Cosignaling of NCAM via lipid rafts and the FGF receptor is required for neuritogenesis. J Cell Biol 157: 521–532.
29. Goswami R, Ahmed M, Kilkus J, Han T, Dawson SA, et al. (2005) Differential regulation of ceramide in lipid-rich microdomains (rafts): antagonistic role of palmitoyl:protein thioesterase and neutral sphingomyelinase 2. J Neurosci Res 81: 208–217.
30. Kielar C, Wishart TM, Palmer A, Dihanich S, Wong AM, et al. (2009) Molecular correlates of axonal and synaptic pathology in mouse models of Batten disease. Hum Mol Genet 18: 4066–4080.
31. Soyombo AA, Hofmann SL (1997) Molecular cloning and expression of palmitoyl-protein thioesterase 2 (PPT2), a homolog of lysosomal palmitoyl-protein thioesterase with a distinct substrate specificity. J Biol Chem 272: 27456–27463.
32. Gupta P, Soyombo AA, Atashband A, Wisniewski KE, Shelton JM, et al. (2001) Disruption of PPT1 or PPT2 causes neuronal ceroid lipofuscinosis in knockout mice. Proc Natl Acad Sci U S A 98: 13566–13571.
33. Patel NH (1994) Imaging neuronal subsets and other cell types in whole-mount Drosophila embryos and larvae using antibody probes. Methods Cell Biol 44: 445–487.
34. Chu-LaGraff Q, Schmid A, Leidel J, Bronner G, Jackle H, et al. (1995) huckebein specifies aspects of CNS precursor identity required for motoneuron axon pathfinding. Neuron 15: 1041–1051.